Response to Review 1

REVISED VERSION according to the Editors decision:
- Changes to the first version highlighted using a bold font.
- Details of changes made to the Discussion version are highlighted in this document by using an underline font.

René Hommel* et al.
* Institute of Environmental Physics, University of Bremen

17 March 2015

We thank the referee for her/his thoughtful comments and suggestions for improvements. We critically revised the manuscript and think that the manuscript has significantly improved after the comments and suggestions have been considered.

In the following, we respond to individual comments. Original remarks of the referee have been enclosed in quotation marks, using an *italic* font. Responses are given below each comment and are marked by "Answer" in a ***bold italic*** font.

Major comments:

"1) It is often difficult to interpret the magnitude of variations in the (color) height vs. time lag plots with small labels (Figs. 4-11), and it is too much work for readers to determine if the variability is large or small. The authors might consider making these plots in % of the respective background values."

Answer: We will carefully revise the figures and increase the font size relative to the size of the figures.

Regarding the 2nd part of this comment we like to state the following: During times of manuscript preparation we carefully elaborated the presentation form of the figures. We also tested whether it makes sense to show composite plots in relative units. Finally we decided to present anomalies in absolute values and denote their relative strength in the respective paragraphs, where the figures and the mechanisms of the individual QBO modulations are discussed. Our decision is based on the following reasons:

1) QBO induced anomalies in stratospheric parameters are commonly presented in absolute terms within diagrams, and we would like to use this common approach. This is in particular true for the composite plots like those we are showing.
2) When the composites are presented in relative units, the colour shading of quite a few figures will change with the result, that the visual impression of these plots ("guiding the eye by colours") in quite a few figures generates a message which is even more difficult to explain as in the current form, focussing on absolute units. For example, QBO anomalies in the aerosol effective radius are small below 20 hPa (Fig. 7b). Using the red-white-blue colour shading, which is commonly used to illustrate anomalies, would largely suppress the existence of the induced anomalies in this region. The shading would then be simply too bright and too close to the zero line so that the very first visual impression is "no effect". But in absolute quantities it is clear that this is indeed not the case. It would also be misleading if one attempts to interpret how the QBO modulates the different processes, which determine an integrated quantity like the effective radius. After a very critical examination of our results we decided to withdraw all composites showing relative units in favour of well described relationships in the respective sections. **However, we describe the relative strength of the anomalies in detail in each section where anomalies are discussed. We show exact numbers or respective ranges in relative units (%).**
3) We also checked whether it would help to show such plots in relative units in an additional panel on the right hand side of each figure from Fig. 4 - 11. However, we felt the information content of those figures did not increase - instead, it rather led to confusion due to that what we explained in 2).

"2) I had difficulty in understanding the take-home message of the CCMI data results in Fig. 6. Both the climatological mean and the composited QBO variability are substantially different from the model results in Fig. 5. I do not worry about the statistical significance of the model results because the QBO is the dominant variability, but I am less convinced about the observed data, where the patterns look confusing

and noisy. Can the authors evaluate the statistical significance of the QBO variations in Fig. 6b, and critically assess the ability of these data to constrain the model results?"

Answer: We revised the CCMI dataset and indeed it turned out that we made a mistake in the calculation of the anomalies. We replace Fig. 6b by an anomaly composite plot, which is less patchy. Now the SAD anomalies in CCMI between 1996 and 2006 are much closer to our model results. The largest improvement is found in the transition periods from QBO east to west phase, where CCMI SAD anomalies are now negatively modulated below approx. 15 hPa. This behaviour is very similar in our model (Fig. 5b and d). Differences remain in regions directly above the TTL, which presumably is due to volcanic influence in the last 3 years of the analysed time-series. In the revised manuscript **we further discuss** the differences of the two data sets (model and observation), **and point to** the importance of the potential volcanic signature in the observations. **Changes affect paragraphs 7-9 in Sec. 3.2.1.**

Regarding differences in the mean SAD, **we improve** our discussion to make clear why the data sets generally differ from each other. **Main reason here is that the volcanic signature is clearly evident in the observations, but is per definition not considered in the simulation.** Please note that the analysis of the climatological mean states was in the focus of our companion paper, Hommel et al. 2011, where we compared model results with two SAGEII data sets. Here, we are using the gap filled and extrapolated CCMI data set (Arfeuille et al., 2013) which is a merger between ERBS/SAGEII and Calipso/CALIOP measurements (CALIOP in the last 1.5 years of the analysed time period). This has been mentioned in our manuscript on page 16258.

Furthermore, we add a paragraph about the statistical significance of the inferred anomalies in model data as well as in the CCMI SAD **(Sect. 3.2.1, paragraphs 4, 6 and 9)**. **In addition, we** performed Student t-test's for all model parameters relative to our reference simulation (Hommel et al., 2011). **For the observational data from CCMI and MIPAS we applied** the F-test against the theoretical red noise spectrum as an appropriate model of variability for a wide range of atmospheric parameters (e.g. Gilman et al, 1963; Yang and Tung, 1994; von Storch and Zwiers, 1999). Significances are now considered in the figures 4-11. The potential volcanic impact in the observed SAD is not only affecting the magnitude and timing of the derived anomalies, it also leaves an imprint in their statistical significance.

"3) The overall results are probably intuitive to experts on stratospheric aerosols, but less so to the general reader. It might help to complement the Discussion section with a summary figure or cartoon highlighting the important aerosol processes and their physical links identified in this study. What are the explicit 'non-linear relationships' mentioned in the Abstract and Discussion section?"

Answer: **We revised** the paragraphs discussing the interactions of the aerosol processes (affecting whole Sec. 3) in order to highlight that the processes are not linearly coupled. To elaborate this a little bit further, this means nothing else than that small relative deviations in one aerosol process due to the QBO (within a certain altitude range) may cause inhomogeneous anomalies in a different aerosol parameter (within the same altitude range). In addition, they may also trigger other aerosol processes, in turn affecting the latter parameter. With the current state of analysis we hesitate to call this process "feedback", because more in-depth studies are needed to clarify how the processes are coupled due to the three major pathways of potential QBO imprints in stratospheric aerosol: advection (of aerosol and precursors), microphysics (in particular nucleation and mass transfer of H2O and H2SO4) and chemistry of precursors. As we state in our manuscript, the simulated aerosol was not coupled to radiation and the full stratospheric chemistry, which would induce more pathways for the QBO to affect the Junge layer.

We agree with the referee and think it is a good idea to sketch the relationships. **After carefully examining the options, we could not find a suitable form to sketch our results in a such a simplified manner that the figure would not raise questions. The basic problem is, that in our opinion such a cartoon should contain all the different QBO-aerosol relationships as described in the manuscript. If we present only parts of our message in such a sketch and neglect other relationships (because they are too complicated to illustrate) we would provide a picture which is not clear enough and the sketch would satisfy only a minority of the readers. Also, putting too much information into one figure may lead to confusion, so that we decided to withdraw our attempt to sketch the processes.**

Instead, we further improved the description of the relationships, made it even more clear and simple as in the Discussion version of the manuscript. We ask that you take this into consideration.

With respect to non-linear relationships, we carefully rephrased respective statements. Changes affect the abstract and in the Conclusions (Sect.4, paragraph 6), but also in the new additional sub-Section 3.6 (Size distribution) we explain those non-linearities.

"4) p. 16255, lines 1-2: it is not easy to identify the 5 km height difference in aerosol mixing ratio in Fig. 3. One suggestion might be to add a figure simply comparing the vertical profiles of mixing ratio for snapshots of QBO east and west phases."

Answer: **We added a new figure (Fig. 5b) which shows the relationship. We found that profiles are not best illustrating the altitude modulation of the Junge layer. Instead, we composited the geometric altitude of the 0.25 ppbm mixing ratio isopleth, compared with the layer thickness between the two 0.25 ppbm isopleth in the regions of the upper and lower "boundaries" of the Junge layer. To be more precise, these data have been converted directly from the model's sigma-hybrid levels and were not approximated by interpolation from pressure levels.**

"5) Regarding the ozone QBO above 20 hPa: because the ozone photochemical lifetime is short above this level, ozone chemistry is important or dominant in this region, rather than the direct effects of transport (transport influences species such as NOy, which in turn influence ozone)."

Answer: We agree with the referee and revise respective sections. **We changed lines 290 to approx. line 300 of the Discussion version of the manuscript to better explain why we refer to the ozone-QBO relationship in the respective section. We focus on the advective component of the QBO in ozone in order to not confuse the reader because our model was not coupled to ozone chemistry.**

"6) p. 16261, line 2: 'interfere' rather than 'infer'? "

Answer: Typo. **It is** corrected.

"7) In addition to Fig. 8, it might be useful to show the aerosol size distributions for extreme QBO phases (perhaps at one or two altitudes where the changes are large)."

Answer: We agree with the referee that this improves the understanding on how the processes influence the size distribution. **We added a section (Sec. 3.6) and a figure (Fig. 13 with four panels) and describe the modulations in detail.**

"8) I could not find any reference or discussion of the DMS results in Figs. 11 e-f."

Answer: Thank you for pointing this out. The Figure should have been removed already in the submitted manuscript **- and is removed now.** DMS is a very minor sulphate precursor in the stratosphere (Weisenstein et al, 1997; SPARC ASAP, 2006; Hommel et al., 2011), and the QBO is not affecting its mixing ratio distinctly. Therefore, we decided to remove the Figure.

References

Arfeuille, F., Luo, B. P., Heckendorn, P., Weisenstein, D., Sheng, J. X., Rozanov, E., Schraner, M., Brönnimann, S., Thomason, L. W., and Peter, T.: Modeling the stratospheric warming following the Mt. Pinatubo eruption: uncertainties in aerosol extinctions, Atmos. Chem. Phys., 13, 11221-11234, doi:10.5194/acp-13-11221-2013, 2013.

Gilman, D.L., Fuglister, F.J., Mitchell, J.M. Jr., On the Power Spectrum of "Red Noise", J. Atmos. Sci., 20, 182-184, 1963. **(added to manuscript)**

Hommel, R., Timmreck, C., and Graf, H. F.: The global middle-atmosphere aerosol model MAECHAM5-SAM2: comparison with satellite and in-situ observations, Geosci. Model Dev., 4, 809–834, doi:10.5194/gmd-4-809-2011, 2011.

SPARC ASAP, WMO/SPARC Scientific Assessment of Stratospheric Aerosol Properties (ASAP), WCRP-124 WMO/TD-No. 1295, SPARC Report No. 4, edited by: Thomason, L. and Peter, T., WMO,2006;.

von Storch and Zwiers, Statistical analysis in climate research, Cambridge University Press, Cambridge, 1999. **(added to manuscript)**

Weisenstein, D. K., Yue, G. K., Ko, M. K. W., Sze, N.-D., Rodriguez, J. M., and Scott, C. J.: A two-dimensional model of sulfur species and aerosols, J. Geophys. Res., 102, 13019–13035, 1997.

Yang, H. and Tung, K.K., Statistical significance and pattern of extratropical QBO in column ozone, Geophys. Res. Lett., 21, 2235-2238, 1994.

Response to Review 2

REVISED VERSION according to the Editors decision:
- ***Changes to the first version highlighted using a bold font.***
- ***Changes to the second version according the Editor's suggestion are highlighted using a red bold font.***
- ***Details of changes made to the Discussion version are highlighted in this document by using an underline font.***

René Hommel* et al.
* Institute of Environmental Physics, University of Bremen

02 April 2015

We thank the referee for her/his thoughtful comments and suggestions for improvements. We revised the manuscript critically and think that the manuscript has significantly improved after the comments and suggestions have been considered.

In the following, we respond to individual comments. Original remarks of the referee have been enclosed in quotation marks, using an *italic* font. Responses are given below each comment and are marked by "Answer" in a ***bold italic*** font.

Major comments:

"1) I think it would be useful to compare the magnitude of the stratospheric aerosol variations due to QBO to that of seasonal variability , annual variability, and volcanic influences. For instance, how much stronger is QBO than seasonal or annual (e.g. tape recorder) variations on stratospheric aerosol? Does the QBO phase impact aerosol properties more than recent volcanic eruptions in the lower stratosphere? upper stratosphere? This could be included in the abstract and some discussion and particularly the conclusions."

Answer: Focus of our manuscript is the examination of QBO influences on aerosol microphysics. It is not our attempt to explain the time-series of tropical stratospheric aerosol in the recent past, which is largely contaminated by volcanic material, in particular beyond 2003 (e.g. Neely et al., 2013). Therefore, it is important to relate the strength of the QBO modulations to the strength of other variabilities or modulations which may affect the analysed aerosol properties. In this respect we agree to the referee. In the revised manuscript we add **a figure** (Fig. 4) showing the comparison between the amplitudes of the annual cycle and the QBO. Also referring to Review #1, **we revised** Section 3.2.1. where we compare our modelled SAD to observations (CCMI data set) and consider estimates of statistical significances and discuss the influence of the volcanic signature in the CCMI SAD in greater detail. That is, of course, an important point, which will be mentioned also in the abstract and the conclusions.

"2) the recent SO2 observations by Hopfner et al which included the contributions of QBO phase is a very relevant comparison to your model. It would be useful to conduct a more detailed comparison between the ranges observed by Hopfner et al and your model, provide a more detailed description of this dataset in your introduction and/or section 2.2, and compare seasonal, annual and QBO-induced variability between the model and dataset."

Answer: We agree with the referee. In the revised manuscript we consider an analysis of MIPAS SO_2 (Hoepfner et al., 2013) in a consistent manner, as done for the model and the observation-based CCMI SAD data set. **More precisely, we added sentences and paragraphs about MIPAS in the sections 1 (Introduction), 2.2. (Observational Aerosol Data), 3.7 (Precursor Gases) and 4 (Conclusions). In Sec. 3.7 we also added Fig. 14c, showing QBO anomalies in MIPAS SO_2, and added the MIPAS profile and the statistical significance estimate of the anomalies to Fig. 14a. The ralated discussion is found in Sect. 3.7.**

"3) There are many places in the paper where you provide qualitative terms like "strongly", "more or less", "substantially smaller", "QBO effect exceptional", "indicates to a certain extent", "heavily influenced" and "rather in-phase" etc. It would be useful to provide more quantitative terms such as x % larger or smaller in x region."

Answer: In the revised manuscript **we avoid** to use those qualitative terms and consolidate our interpretation by referring to relative quantities where appropriate. **More precisely, in each paragraph discussing QBO anomalies we now state the relative strength of the signal in relative units (%).**

"4) There are also many places in the paper with grammatical errors and typos. I've tried to list most of them in my specific comments but please double check other places."

Answer: We thank the referee for several corrections and comments on typographic and grammatical problems. **We have corrected all typos and errors we found.**

"5) How might contributions from aerosols that you don't include in these simulations convolute your analyses? Please provide some discussion around that. For instance meteoritic dust contributes significantly to upper stratospheric aerosol (see Neely et al., 2011), and recent volcanic eruptions (Vernier et al 2011) and other aerosol species such as carbon (Murphy et al 2007) contribute to lower stratospheric aerosol ."

Answer: With respect to volcanic material, we cannot neglect that it may leave an imprint in the inferred signatures of the CCMI SAD, a merged SAGEII/CALIOP data set. For the model the relationships are even more clear - there is no direct influence of volcanos considered, as we state clearly in our manuscript and the companion paper Hommel et al., 2011. As mentioned above, and also in our answers to Reviewer #1, in the revised manuscript **we improve** the discussion about the imprint of volcanos in the CCMI SAD **(changes affect Sec. 3.2.1 for SAD but also Sec. 3.7, where MIPAS SO_2 is discussed)**. However, we like to emphasise that the focus of our paper is the QBO-aerosol microphysics relationship and not an analysis of the stratospheric aerosol record as observed in the recent past. In our opinion it is necessary to first understand how aerosol processes are affected by the QBO, which is the dominant natural forcing in the lower tropical stratosphere, before the effects from the modulation by precursors with volcanic origin are separated. In this respect our work can be seen as one necessary step towards an in-depth understanding of the lower stratospheric aerosol behaviour as observed in the recent past. **In the conclusions (Sec.4) we state this more clearly now.**

With respect to particulate matter other than sulphate dominated (liquid) particles, we agree to the referee that other studies indicated their relevance for the stratospheric aerosol burden, AOD, radiative forcing etc. But, as said before, we focused on sulphate aerosols, and did not considered other species than H_2O and H_2SO_4 or even other particulate matter because sulphate clearly dominates the stratospheric aerosol mass. Our attempt is to reduce the complexity of the system as far as possible without losing physical meaning. In our opinion this is a common procedure in atmospheric science global model studies. It is beyond the scope of our study to show a complete picture of particulate matter dynamics in the lower stratosphere. Each process and each substance additionally considered would imply a much higher complexity in the relationships to be analysed and making an interpretation very complicated. Another, more technical aspect shall be noted here: we used a computationally relatively expensive aerosol scheme (sectional approach with 35 bins). Extending the scheme to other aerosol classes and mixing states would increase the computational demand beyond a reasonable level. For more complex model studies, e.g. in-detail studies on volcanic effects, other less expensive aerosol schemes are favoured - and succeeded already when coupled to the same host model as used here (e.g. Niemeier et al. 2009).

In this respect we like to mention that this paper presents work in progress. Until now, not much has been published about the detailed mechanisms of the QBO-aerosol microphysics relationship. So far those relationships have been either indicated from aerosol extinction/backscatter observations or have been shown for very few quantities on much shorter time-series from models (Brühl et al., 2012). To address this wide field of lower stratospheric aerosol processes, this study is a first step towards a deeper understanding by utilising a system of reduced complexity.

"6) The discussion of ozone on p16256 is confusing. Are you presenting any of your ozone results here? If not, it seems risky to compare your model's aerosol extinction to observations of ozone and make conclusions regarding the relative changes."

Answer: We do not show ozone. And, we have to correct the reviewer, we do not show aerosol extinctions either. Our attempt here was to point out that the QBO-aerosol relationship is nothing special related to aerosol exclusively. Instead most of the mechanism's exist for most of the trace constituents in the lower stratosphere. We have chosen the example ozone because the ozone-QBO relationship is the best explored and discussed in a variety of articles. We carefully **revised** the section **(Sec. 3.1.2, affecting lines 290 to approx. line 300 of the Discussion version of the manuscript**) **in order to** make clear why ozone is simply an analogy. Although the magnitude of the QBO modulations in the mixing ratios of aerosol and ozone is approximately similar, we cannot prove in our study whether it arises from the same mechanisms which dominate the modulations.

"7) I find it a little concerning that your section 3.4 Microphysical processes ignores coagulation and sedimentation. Aerosol microphysical processes occur together in complex ways, and for instance coagulation and sedimentation can alter the rates of condensational growth and evaporation. Perhaps you could devote some discussion as to the caveats of your approach in section 3.4."

Answer: We thank the referee for mentioning this point. During the time of manuscript preparation we critically examined whether it makes sense to describe potential QBO effects in sedimentation and coagulation. We did not diagnosed both processes in a way making such a comparison meaningful (stated on page 16262 lines 23-26). We decided to withdraw the two sections about coagulation and sedimentation. Let us explain in a few words the reasons: Sedimentation, for instance, is diagnosed in terms of the sedimentation velocity for each aerosol bin that has been defined in the microphysics scheme and as an accumulated flux at the surface. Both parameters are not suitable to examine QBO effects. Since we did not have an appropriate measure to quantify coagulation, the process has not been diagnosed during model integration. An offline diagnostics also does not seem possible, because it cannot separate the competing size distribution shaping processes from each other. This could be achieved by sensitivity studies, switching on/off the microphysical processes, for instance, but such experiments have not been conducted so far and are subject of future research.

We carefully revised Sec. 3.4. We added a new sub-Section (Sec. 3.4.4) where we discuss potential QBO effects in the processes sedimentation and coagulation based on our model results and simple relationships of aerosol dynamics (e.g. Seinfeld and Pandis, 2006).

Specific items:

Basically, many of the other comments the referee listed under 'Specific items' refer to linguistic problems of the manuscript. We have considered carefully each of the remaining comments in the revision. We very much appreciate the valuable suggestions of the referee.

The more content specific comments are answered below:

"Abstract: Please quantify the relationship between QBO and the anomalies. Instead of saying that the aerosol load is "predominately influenced by QBO-induced anomalies...", please state the relationship (easterly-phase causes xxxx to happen). Instead of saying "large impacts are seen" quantify the percentage change from one QBO phase to the other."

Answer: We agree with the referee and **rephrased** the abstract.

"p16244 line26: change "is influenced by" to "may be influenced by" (since for example Neely et al 2013 found very little contribution of asian aerosol to the stratospheric aerosol)"

Answer: This is correct. The sentence has been rewritten.

"p16345 line 15: Please provide more details with regards to "These problems are addressed in the current study". perhaps something along the lines of: "In this study we propose to quantify the contributions of QBO to changes in stratospheric concentrations of background aerosols and their precursors.""

Answer: We agree with the referee. **We changed the sentence into: "Our study addresses in particular the latter issues as we will explain below." (Sect. 1, 2nd paragraph, last sentence).**

"p16246 line 19, 21: Add English et al., 2013 citation to the sentence describing Pinatubo studies using size-resolved models, and Campbell et al 2014 to the list of citations for background aerosol."

Answer: We thank the referee for pointing us towards the Campbell et al. paper, which we didn't consider in the manuscript so far. In order to complete the list of models resolving the size of stratospheric aerosol, in the revised manuscript we will also refer to volcanic studies and cite e.g. the English et al. paper.

"p16246 line 22: Be more specific in the "In this study" sentence, describing that you are mainly focusing on the impacts of QBO on stratospheric dynamics and aerosol."

Answer: We agree with the referee and make the sentence more clear in the revision. **The changed paragraph reads as follows:**
"In this study we address certain aspects of the coupling between stratospheric dynamics and aerosol microphysical processes, as they are important to understand the contributions of QBO and natural variability to recent observed changes of stratospheric aerosol, and as they are key to evaluate stratospheric geoengineering options. We focus on effects imposed by the quasi-biennial oscillation (QBO) in the tropical stratosphere (reviewed in Baldwin et al., 2001) as this dominant mode of stratospheric variability largely impacts the global dispersion of stratospheric trace constituents (e.g. Gray and Chipperfield, 1990}. In particular we address the QBO signatures in the aerosol mixing ratio, in the integral and resolved aerosol size as well as in the abundance of aerosol precursors. Furthermore, we estimate the QBO signal in microphysical processes determining the transfer of sulphur mass between the gas and aerosol phases, i.e. nucleation and condensation/ evaporation. "

"p16246 line 24: In addition to geoengineering, this work is valuable to understand the contributions of QBO and natural variability to recent observed changes to stratospheric aerosol."

Answer: This is true, **we considered** this suggestion. **Please find detailed changes in the answer above.**

"p16248 line 19: 39 levels is somewhat coarse to capture stratospheric dynamics. Have you conducted any studies to determine whether the vertical resolution is sufficient to capture stratospheric processes?"

Answer: QBO nudging greatly improves the representation of stratospheric dynamics. Without QBO nudging, tracer transport in the vertically coarse 39 layer model has strong deficits which arise mainly from too strong upwelling (see also Giorgetta et al., 2006). Our model configuration has been tested against the free-running, the QBO not reproducing, model version in some more detail. Results were published as a technical note in Hommel (2008; in German only). As shown there, the behaviour of the water vapour tape recorder was greatly improved in the QBO-nudged model, being in good agreement with the vertically much higher resolved 90 layer version of the host model. That gave us the confidence that we found an appropriate setup up to conduct our aerosol experiment. We didn't test the 90 layer version of the model, simply because during the time we conducted the studies we did not have the computational resources to perform a companion long-term integration with the higher resolved version coupled to this expensive microphysics scheme. It is true that technical advances have not stopped in the meantime. And, like other middle-atmosphere GCMs, also our host model underwent development, and the capacities of computational facilities increased rapidly. Nowadays, one could perform further studies on the subject with a free-running (i.e. no nudging) and higher resolved model, and also coupled to chemistry (see Neely et al. 2013; Dhomse et al., 2014).

"p16249 line 20: What are prescribed "climatological" oxidant fields? Do they include the variations in stratospheric concentrations due to QBO? If not, it would be useful to quantify how much they vary between different phases of QBO, and how that might impact your model results."

Answer: ~~We thank the referee for this objection. Here, we refer to the climatological means of monthly mean oxidant mixing ratios derived from a long-term integration of the chemistry climate model MESSy (Jöckel et al., 2005). More details are given in Hommel et al., 2011. We revised the paragraph carefully in order to make clear that we coupled sulphur chemistry to the aerosol module, which is not an interactive full chemistry scheme. Therefore, the oxidant fields are needed.~~ **~~Changes affect Sec. 2.1, last two paragraphs. Two new references have been added (Horowitz et al, 2003, and Jöckel et al, 2005).~~**

Answer: We thank the referee for this objection. Here, we refer to the climatological means of monthly mean oxidant mixing ratios derived from a long-term integration of the **chemistry transport model MOZART2 (Horowitz et al., 2003)**. More details **about the model setup** are given in Hommel et al., 2011. **In the climatological average, direct QBO signatures are no longer present in the monthly mean fields. We expect that an explicit consideration of respective QBO signatures would lead to stronger variations in the simulated aerosol precursors due to the QBO. And, hence in the prognostic aerosol mixing ratio. Presumably also in other aerosol parameters we analysed. The numerical study of Brühl et al. (2012), also being discussed in our manuscript, gives evidence for a direct coupling between stratospheric chemistry cycles and interactively coupled aerosols. But to our knowledge the QBO modulation of the oxidising pathway from sulphate aerosol precursors to aerosols (via at least O_3, OH, O(3P) and NO_2) has not been quantified in peer reviewed literature. In the revised manuscript we consider this point in Sect. 3.7, last paragraph, lines 915ff, and in the Conclusions (Sect. 4), line 967ff. We also added two new references in Sect. 2.1, lines 175-177: Horowitz et al, (2003) for MOZART2 and Jöckel et al. (2005) for MESSy.**

"p16249 line 28: why does it take 6 years to reach steady state? stratospheric lifetime is typically a year or 2."

Answer: This is true. But the model needs a few years longer to achieve equilibrium state because it was initialised based on the climatological mean zonal mean SAGEII volume density (University of Oxford retrieval, Wurl et al., 2010). More details on the basic experiment design are given in Hommel et al. 2011. It shall be noted that more details about the spin-up procedure are described in the technical note of Hommel (2008; in Germany only). Alternatively, one could initialise the model from scratch, i.e. no aerosols initialised. Then the aerosol is formed from the emission and it will need more than a decade until they have been well mixed in the atmosphere (we estimated 1.5*maximum of mean age of air in the stratosphere is the required minimum spin up time for such a case). **Changes affect last paragraph of Sec. 2.1.**

"p16250 line 4: Describe the specific "aerosol forcing data set" you are referring to. Extinctions? SAD?"

Answer: Thank you for pointing this out. In the revised manuscript, it is now stated that the forcing data set consist of SAD **(changes affect Sec. 2.2, 1st paragraph)**.

"p16253 lines 14+: this paragraph could use more citations."

Answer: We agree with the referee and and consider additional citations. **We additionally cite Holton et al (1995), Baldwin et al. (2001), Fueglistaler et al. (2009), and Andrews et al. (1987) in the 5th paragraph of Sec. 3.1.1.**

"p16257 lines 1-4: It is important to take what into account? condensational growth? Is this more important that coagulation? It seems that several microphysical properties are important."

Answer: We thank the referee to point this out. We **rephrased** the paragraph **(Sec. 3.2.1, 1st paragraph)** in order to state more clearly, that biases between model and remotely sensed integrated aerosol size quantities may be easily introduced, when in the calculation of the model parameters the model's aerosol size range is not adopted to the detection range of the instrument.
The changed paragraph reads as follows:

"Integrated aerosol parameters inferred from observed aerosol extinction coefficients at specific wavelength are fraught with uncertainties when the fraction of small particles significantly contributes to an aerosol size distribution (Dubovik et al., 2000; Thomason et al., 2008). SPARC/ASAP (2006) emphasised that this effect is particularly relevant when the aerosol load of the stratosphere is low. HOM11 showed that a systematic bias between observations and the CTL simulation arises in integrated aerosol size quantities when H_2SO_4 condensation dominates the growth of LS aerosols. Thus, in comparisons between integrated aerosol size quantities from models and remote sensing, particular attention should be paid to the systematic bias that is due to the fine mode fraction of aerosol populations."

"p16257 line 5: please quantify "strongly depends". For instance something like "including particles smaller than xx nm increases SAD by xx %""

Answer: We agree with the referee and **rephrased the paragraph (Sec. 3.2.1, 2 & 3rd paragraph) and changed also other paragraphs where such inappropriate formulations were used.**

"p16257 lines 14-15: I don't believe that larger particles evaporate at higher rates than small particles. As large particles start to evaporate they become small particles. Please clarify."

Answer: We agree with the referee. This is misleading and has been removed from the manuscript **(Sec. 3.2.1, 2 paragraph**).

"p 16257 line 22: do you mean greater than 0.005 um instead of less than?"

Answer: This is correct, it is a typo **and is corrected.**

"p16258 lines 12-20: how does your modeled SAD compare to SAGE when you cutoff particle size smaller than the detection limit of SAGE?"

Answer: The bias to SAGEII would be even more pronounced when more fine mode aerosols are considered in the SAD integral of the model. In our companion paper we show this effect for the effective radius compared to measurements from the University of Wyoming optical particle counter (Hommel et al., 2011; Fig. 13).

"16259 line 18: negatively biased to what kind of observations – satellite or aircraft? Satellite observations have known biases as you've stated but aircraft observations are more reliable"

Answer: This sentence refers to SAGE II observations based on the climatologies provided by the University of Oxford (Wurl et al, 2010) and NASA AMES (Bauman et al., 2003a,b). The sentence has been rewritten**:** **"Although negatively biased to the SAGE II climatologies of Bauman et al. (2003a,b,) and Wurl et al. (2010) as well as in-situ observations of the balloon-borne optical particle counter of the University Of Wyoming (Deshler et al. 2003), in the control experiment without a QBO, the model predicted R_{eff} lies within the uncertainty range of the measurements (HOM11)."**

"p16261: the paragraph discussing nucleation should probably go before the current preceding paragraph which discusses other microphysics. References"

Answer: We are not entirely sure what the referee means. In our opinion also the nucleation process depends on the water content and the stratospheric temperature, i.e. two key aspects which are mentioned in the introductory paragraph of Sec. 3.4, intended to introduce the chapter about the modelled QBO impact on aerosol microphysics. **We changed the section's structure, now describing the behaviour in the nucleation mode first.**

"p16261 line29: nucleation mode does not prove BHN occurs as other processes such as ion-mediated nucleation may occur. perhaps state that it suggests BHN is occurring."

Answer: We agree with the referee and **rephrased the sentence: "As seen from the nucleation mode number density profile (Fig. 10a), the model suggests that binary homogeneous nucleation (BHN) occurs in the tropical LS. "**

"p16262 line 21: "vapour contents" is not a common way to describe the thermodynamics. Perhaps use the words "supersaturation of h2so4 and water, which depends on temperature and vapor concentration..."

Answer: We agree with the referee and **rephrased the sentence: "The saturation of H_2SO_4 and H2O, which depends on temperature and vapour concentrations, determines the rate of formation of new aerosol as well as their growth and loss through reversible mass transfer between the gas and the liquid phase."**

"p16263 line 9: What do you mean by "can amount to 50%"? under which circumstances?"

Answer: We will rephrase the sentences and more precisely describe the **relationships**: **"Although this is not a large number, the respective increase in the nucleation mode number density can be as large as ± 50 % during times when QBO easterlies are strongest. During that time the layer approaches its lowest vertical expansion, so that the disproportional modulation in the number density of nuclei may arise from dampening the advective aerosol lofting or from QBO-induced downward transport (relative to the climatological mean state). "**

"p16263 line 16: what are the units of time-averaged moleculate concentration transferred? seems like time should be on the denominator, but this is not noted in Fig. 9."

Answer: ~~We diagnosed, as in Hommel et al. (2011), the H_2SO_4 molecule concentration that is transferred between the two phases. Units are molecules per cm^3. This quantity is directly comparable to the 'normal' sulphate concentrations of the liquid and gas phase. Diagnosing this transferred concentration directly helped us a lot to understand how the model behaves, e.g. how the size distribution is shaped in the presence of steep gradients. Diagnosing a rate would have made sense if we would have had other data to compare. But in literature we did not found comparable mass transfer rates of sulphate under representative stratospheric conditions (in contrast to nucleation rates), so that we tried to retain control over the modelled mass transfer process on the molecular level (incl. extensive mass balancing). To our knowledge, also deviations of microphysics process fluxes due to the QBO have not been published so far.~~

Answer: We agree to the reviewer. To avoid misinterpretations we changed the mass transfer quantities of H_2SO_4 vapour. We now show the condensable source rate (in units of molecules cm-3 s-1) and its counterpart, the evaporation sink rate (there is no other appropriate name in literature, to our knowledge). This change does not affect the general message of the two sections and paragraphs where we describe the interplay between H_2SO_4 vapour condensation and evaporation.

"p16264 line 21: does warmer T also explain the changes in saturation vapor pressure above 20 hPa?"

Answer: We are not entirely sure what the referee means. The saturation vapour pressure is modulated by the QBO in an almost linearly manner, under the assumption that no additional gain or loss due to mass transfer occurs.

"p16265 lines 14-19: could the temperature biases affect modeled nucleation and growth in addition to evaporation as you've noted?"

Answer: The referee raises a good point. Nucleation should be affected, yes. Condensational growth theoretically also, but we assume the effect is more critical for evaporation. Because this process limits the upper tail of the Junge layer. And, as we mentioned in our manuscript, this upper tail varies due to the QBO by up to 5 km. Thus, potential temperature biases should affect especially those processes which occur there. We **rephrased** the paragraph, pointing out the importance for the other processes. **The changed paragraph reads as follows:**
"It should be mentioned that compared to the ERA-Interim reanalysis, modelled QBO temperature anomalies are up to 2 K smaller below the 10 hPa pressure level (Fig. 2a, b) and 1-2 K larger above 10 hPa, where evaporation

occurs. Thus, in the model the net effect of QBO on the counteracting processes evaporation and condensation of H_2SO_4 may be overestimated to some degree. On the other hand, due to the large QBO induced variations of the Junge layer's upper lid, presumably temperature-related biases in the modelled QBO interactions are more pronounced for evaporation. That is because the process ultimately determines the maximum altitude of the layer's upper lid, dependent on the saturation state and the thermodynamic stability of aerosol. "

"p16266 line 18: how does QBO "interfere" with the annual cycle?"

Answer: We **considered** additional citations here, and **rephrased** the paragraph **(Sec. 3.5, last paragraph)** to describe the relationships:
"The analysed aerosol properties are also modulated by changes due to seasonal variations in the stratospheric temperature (e.g. Steele and Hamill, 1981; Yue et al., 1994). Since the latter are stronger above the TTL than in the middle stratosphere, seasonal variations in the aerosol properties play a particular role below the evaporation region. For instance, at 70 hPa the sulphuric acid weight percentage and water content vary between summer and winter by about 20 % (not shown), and the density of the droplet solution by ≈6 %. At 10 hPa the variations do not exceed 1-2 %. Hence, below approximately 20 hPa, these variations are up to a magnitude stronger than the inferred QBO signatures. This is clearly different from the aerosol mixing ratio (Fig. 4), where only below 70 hPa seasonal variations are (approximately two times) stronger than the QBO signal."

"p16267 line 27: add Campbell et al 2014 citation."

Answer: We thank the referee for pointing us towards the Campbell et al. paper. We like to state that we did not had knowledge about its existence during time of manuscript preparation. We cite it in the revised manuscript (**Sec. 1, paragraph 5; Sec. 3.7, paragraph 3).**

"p16268 lines 16-25: A more direct comparison between your model SO2 and Hopfner et al would be useful. How do each SO2 vary between QBO phases? how do so2 annual and seasonal variations compare? "

Answer: As mentioned above, we **added** a consistent analysis of MIPAS SO_2 (Hoepfner et al., 2013) **in Sec. 3.7, incl. an additional sub-figure Fig. 14c and additional profiles and significant altitude ranges in Fig. 14a.**

"p16269 lines 17-21: this reasoning is not clear to me. To me, aerosols in the lower stratosphere seem strongly driven by transport from upper troposphere, but aerosols in the middle stratosphere are more driven by OCS oxidation. Please clarify your reasoning."

Answer: The sentence "Together with ... indicates ... to a certain extent ..." **in the Discussion version of the manuscript** refers to the sentence before - or in other words to anomalies in the Aitken mode number density. Which are largely in-phase with SO_2 and H_2SO_4 vapour anomalies up to the 30 hPa pressure level. Additionally, we find also in-phase anomalies in the nucleation mode, and obviously in the nucleation rate, around 50 hPa, which suggest that *not all* of the Aitken mode aerosol in this region has been formed in the free troposphere. Whether the H_2SO_4 vapour at this altitude comes from OCS oxidation or SO_2 is not entirely clear from our model, because we used prescribed OCS mixing ratios (due to the absence of appropriate emission data during time we performed the experiment).

In our perspective, we found a reasonable chain of process modulations here, and do not rule out that fine mode aerosols are transported through the TTL. **We carefully revised** this section in order to avoid misunderstandings. **The changed paragraph reads as follows:**
"Furthermore, modelled QBO anomalies in the two precursor gases are in-phase with modulations in the Aitken mode aerosol number density (Fig. 10d) and the H_2SO_4 vapour condensing onto aerosols (Fig. 11d). This implies that pre-existent or newly formed aerosols rapidly grow by H_2SO_4 condensation, even though the strength of condensation decreases rapidly with height (Fig. 11c). Together with in-phase anomalies in the nucleation rate and nucleation mode number density around 50 hPa, this result indicates that, at least partly, the

origin of Aitken mode aerosols in the LS is not the free troposphere, from where they have been more rapidly uplifted when the QBO phase is easterly. However, we cannot provide an more detailed quantification of pathways maintaining the volcanically quiescent aerosol layer in the tropical stratosphere, because it would require that OCS, one of the major sulphur sources in the LS (e.g. SPARC/ASAP, 2006), needs to be treated prognostically (e.g. Bruehl et al, 2012). "

"p16269 line 26-27: add "and so2 measurements (Hopfner et al 2013).""

Answer: Considered in the revised manuscript **(Sec. 4, 1st paragraph).**

"p16271 lines 24-27: the assumption that condensation and evaporation occur concurrently seems risky. I would suggest that you analyze your instantaneous model output to determine whether this is true, or change your discussion of it."

Answer: We explicitly state "... in the time average ...", at the beginning of the criticised sentence, line 24. It is a fact that during an output time step (6 hours), which is considerably longer than an integration time step (15 minutes), both processes can be diagnosed within the same grid cell. This has to bear in mind when the QBO signatures in the two processes are analysed. Because equally phased anomalies may overlap partially in the residual composites, although condensation and evaporation compete on the process level in the model. Also we like to mention that the output is time-averaged, and not instantaneous. At the beginning we also had some doubts and revised the results several times (also results of the companion simulation, Hommel et al., 2011, where it is similar but less pronounced). We have no indication that this is an error in the diagnostics or the model itself - instead for us it is very plausible mechanism and a straightforward model behaviour.

We changed the beginning of the 6th paragraph of Sect. 4 into:

"The model predicts that the QBO modulates the balance of the mass transfer of H_2SO_4 vapour between the gas and the droplet's liquid phase. The mass transfer is shifted towards evaporation in the QBO-nudged model, compared to the CTL simulation. ..."

"Fig. 2. Why is there a sharp gradient in ERA-interim at 15 hPa?"

Answer: We are not entirely sure what the referee means. We think she/he refers to a horizontal line of colour shades in Fig. 2 a around the 15 hPa pressure level, representing the QBO induced temperature anomaly in the ERA-Interim reanalysis. We revised the data and it seems that the referee refers to a visual impression that arises from the so-called 'blockfill' technique of our post-processor, which fills the area between the data points with their colour-coded cell averages. Below, we reproduced the figure without using the 'blockfill' technique. Instead, here it has been linearly interpolated between the data points. No exceptional vertical gradients in the temperature anomalies can be found.

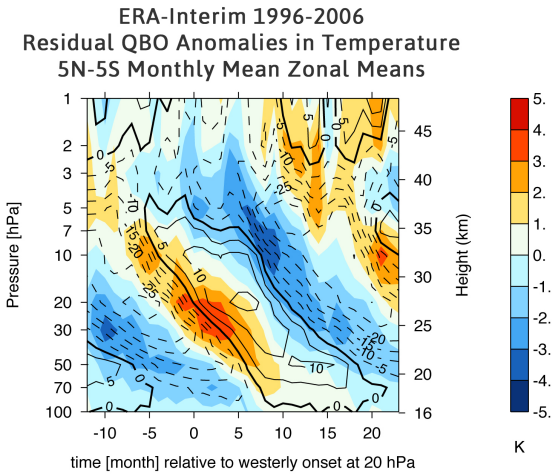

"Fig. 3: I thought your control simulation had prevailing easterly winds? why are there some non-dotted lines (e.g. westerlies)? Also "Ratio" is mis-spelled in the title"

Answer: We thank the referee to point this out. It should be noted in Sec. 3.1.1, and also in Sect. 2.3 'Meteorology' that in the CTL experiment westerly winds of the semi-annual oscillation (SAO) penetrate down from the mesosphere to the 30 hPa pressure level. Fig. 1c is showing these westerlies in reddish colours, enclosed by a continuous black contour line, marking the zero zonal mean wind. The same zonal wind contour lines overlay the aerosol mixing ratio in the CTL experiment, Fig. 3a. We **rephrased** respective paragraphs and describe this model feature. However, the prevailing wind regime in the CTL experiment is easterly (see also Giorgetta et al., 2002).
Changes affect 1st paragraph of Sec. 2.3 (Meteorology), and the 2nd and 3rd paragraph of Sec. 3.1.1 (Temporal evolution).

References

Andrews, D. G., Holton, J. R., and Leovy, C. B.: Middle Atmosphere Dynamics, Academic Press, San Diego, CA, 1987.

Baldwin, M. P., Gray, L. J., Dunkerton, T. J., Hamilton, K., Haynes, P. H., Randel, W. J., Holton, J. R., Alexander, M. J., Hirota, I., Horinouchi, T., Jones, D. B. A., Kinnersley, J. S., Marquardt, C., Sato, K., and Takahashi, M.: The quasi-biennial oscillation, Rev. Geophys., 39, 179–229, 2001.

Bauman, J. J., Russell, P. B., Geller, M. A., and Hamill, P.: A stratospheric aerosol climatology from SAGE II and CLAES measurements: 1. Methodology, J. Geophys. Res., 108, 4382, doi:10.1029/2002JD002992, 2003a.

Bauman, J. J., Russell, P. B., Geller, M. A., and Hamill, P.: A stratospheric aerosol climatology from SAGE II and CLAES measurements: 2. Results and comparisons, 1984–1999, J. Geophys. Res., 108, 4383, doi:10.1029/2002JD002993, 2003b.

Brühl, C., Lelieveld, J., Crutzen, P. J., and Tost, H.: The role of carbonyl sulphide as a source of stratospheric sulphate aerosol and its impact on climate, Atmos. Chem. Phys., 12, 1239–1253, doi:10.5194/acp-12-1239-2012, 2012.

Campbell, P., M.Mills, and T. Deshler, The global extent of the mid stratospheric CN layer: A three-dimensional modeling study, J. Geophys. Res. Atmos., 119, 1015–1030, doi:10.1002/2013JD020503, 2014.

Dhomse, S. S., Emmerson, K. M., Mann, G. W., Bellouin, N., Carslaw, K. S., Chipperfield, M. P., Hommel, R., Abraham, N. L., Telford, P. , Braesicke, P., Dalvi, M., Johnson, C. E., O'Connor, F., Morgenstern, O., Pyle, J. A., Deshler, T., Zawodny, J. M., Thomason, L. W., Aerosol microphysics simulations of the Mt. Pinatubo eruption with the UM-UKCA composition-climate model, Atmos. Chem. Phys., 14, 11221--11246, 10.5194/acp-14-11221-2014, 2014.

English, J. M., O. B. Toon, and M. J. Mills, Microphysical simulations of large volcanic eruptions: Pinatubo and Toba, J. Geophys. Res. Atmos., 118, 1880–1895, doi:10.1002/jgrd.50196, 2013.

Fueglistaler, S., Dessler, A. E., Dunkerton, T. J., Folkins, I., Fu, Q., and Mote, P.W.: Tropical tropopause layer., Rev. Geophys., 47, RG1004, doi:10.1029/2008RG000267, 2009.

Giorgetta, M. A., Manzini, E., Roeckner, E., Esch, M., and Bengtsson, L.: Climatology and forcing of the quasi-biennial oscillation in the MAECHAM5 model, J. Climate, 19, 3882–3901, 2006.

Giorgetta, M. A., E. Manzini, and E. Roeckner, Forcing of the quasi-biennial oscillation from a broad spectrum of atmospheric waves, Geophys. Res. Lett., 29(8), doi:10.1029/2001GL014756, 2002.

Höpfner, M., Glatthor, N., Grabowski, U., Kellmann, S., Kiefer, M., Linden, A., Orphal, J., Stiller, G., von Clarmann, T., Funke, B., and Boone, C. D.: Sulfur dioxide (SO2) as observed by MIPAS/Envisat: temporal development and spatial distribution at 15–45 km altitude, Atmos. Chem. Phys., 13, 10405–10423, doi:10.5194/acp-13-10405-2013, 2013.

Hommel, R.: Die Variabilität von stratosphärischem Hintergrund- Aerosol, Eine Untersuchung mit dem globalen sektionalen Aerosolmodell MAECHAM5-SAM2, Berichte zur Erdsystemforschung, Reports on Earth system science, Max Planck Institute for Meteorology, Hamburg, 2008.

Hommel, R., Timmreck, C., and Graf, H. F.: The global middle-atmosphere aerosol model MAECHAM5-SAM2: comparison with satellite and in-situ observations, Geosci. Model Dev., 4, 809–834, doi:10.5194/gmd-4-809-2011, 2011.

Holton, J. R., Haynes, P. H., McIntyre, M. E., Douglass, A. R., Rood, R. R., and Pfister, L.: Stratospheric–tropospheric exchange, Rev. Geophys., 33, 403–439, 1995.

Horowitz, L. W. and S. Walters and D. L. Mauzerall and L. K. Emmons and P. J. Rasch and C. Granier and X. X. Tie and J. F. Lamarque and M. G. Schultz and G. S. Orlando and G. P Brasseur, A global simulation of tropospheric ozone and related tracers: Description and evaluation of MOZART, Version 2, J. Geophys. Res., 108, 2003.

Jöckel, P., Sander, R., Kerkweg, A., Tost, H., and Lelieveld, J.: Technical Note: The Modular Earth Submodel System (MESSy) – a new approach towards Earth System Modeling, Atmos. Chem. Phys., 5, 433–444, doi:10.5194/acp-5-433-2005, 2005.

Niemeier, U., Timmreck, C., Graf, H.-F., Kinne, S., Rast, S., and Self, S.: Initial fate of fine ash and sulfur from large volcanic eruptions, Atmos. Chem. Phys., 9, 9043–9057, doi:10.5194/acp-9-9043-2009, 2009.

Neely, R. R. I., Toon, O. B., Solomon, S., Vernier, J.-P., Alvarez, C., English, J. M., Rosenlof, K. H., Mills, M. J., Bardeen, C. G., Daniel, J. S., and Thayer, J. P.: Recent anthropogenic increases in SO2 from Asia have minimal impact on stratospheric aerosol, Geophys. Res. Lett., 40, 1–6, doi:10.1002/grl.50263, 2013.

Seinfeld, H. J. and S. N. Pandis, Atmospheric chemistry and physics: From air pollution to climate change., 2nd ed, Wiley-Interscience, New York, 2006.

Wurl, D., Grainger, R. G., McDonald, A. J., and Deshler, T.: Optimal estimation retrieval of aerosol microphysical properties from SAGE II satellite observations in the volcanically unperturbed lower stratosphere, Atmos. Chem. Phys., 10, 4295–4317, doi: 10.5194/acp-10-4295-2010, 2010.

Manuscript prepared for J. Name
with version 2.3 of the LaTeX class copernicus.cls.
Date: 3 April 2015

Quasi-biennial oscillation of the tropical stratospheric aerosol layer

René Hommel[1,*], Claudia Timmreck[1], Marco A. Giorgetta[1], and Hans F. Graf[2]

[1]Max Planck Institute of Meteorology, Hamburg,Germany
[2]Department of Geography, Centre for Atmospheric Science, Cambridge University, Cambridge, UK
[*]now with: Institute of Environmental Physics (IUP), University of Bremen, Bremen, Germany

Correspondence to: rene.hommel@iup.physik.uni-bremen.de

Abstract. This study describes how aerosol in an aerosol-coupled climate model of the middle atmosphere is influenced by the quasi-biennial oscillation (QBO) during times when the stratosphere is largely unperturbed from volcanic material. ~~In accordance with satellite observations, the tropical stratospheric aerosol load is predominately influenced by QBO induced anomalies in the vertical advection. Large impacts are seen in the size of aerosols, in particular in the region where aerosol evaporates. This turns the quasi-static balance between processes maintaining the vertical extent of the Junge layer in the tropics into a cyclic balance when considering this dominant mode of atmospheric variability.~~ **In accordance with satellite observations, the vertical extent of the stratospheric aerosol layer in the tropics is modulated by the QBO by up to 6 km, or ∼35 % of its mean vertical extent between 100–7 hPa (about 16–33 km). Its largest vertical extent lags behind the occurrence of strongest QBO westerlies. The largest reduction lags behind maximum QBO easterlies. Strongest QBO signals in the aerosol surface area (30 %) and number densities (up to 100 % e.g. in the Aitken mode) are found in regions where aerosol evaporates, that is above the 10 hPa pressure level (∼31 km). Positive modulations are found in the QBO easterly shear, negative modulations in the westerly shear. Below 10 hPa, in regions where the aerosol mixing ratio is largest (50–20 hPa, or ∼20–26 km), in most of the analysed parameters only moderate statistically significant QBO signatures (<10 %) have been found. QBO signatures in the model prognostic aerosol mixing ratio are significant at the 95 % confidence level throughout the tropical stratosphere where modelled mixing rations exceed 0.1 ppbm. In some regions of the tropical LS the QBO signatures in other analysed parameters are partly not statistically significant. Peak-to-peak amplitudes of the QBO signature in the prognostic mixing ratios are up to twice as large as seasonal variations in the region where**

aerosols evaporate and between 70–30 hPa. Between the tropical tropopause and 70 hPa the QBO signature is relatively weak and seasonal variations dominate the variability of the simulated Junge layer. QBO effects on the upper lid of the tropical aerosol layer turn the quasi-static balance between processes maintaining the layer's vertical extent into a cyclic balance when considering this dominant mode of atmospheric variability. Global aerosol-interactive models without a QBO are only able to simulate the quasi-static balance state. To assess the global impact of stratospheric aerosols on climate processes, those partly non-linear relationships between the QBO and stratospheric aerosols have to be taken into account.

1 Introduction

The stratospheric aerosol layer, also referred to as the Junge layer (Junge et al., 1961), is a key constituent in the Earth's atmosphere. The Junge layer plays an important role in the determination of the Earth's radiation budget and interacts with the cycles of chemically-induced ozone depletion in the polar winter stratosphere. It is generally believed to be maintained by the oxidation of tropospheric Sulphur Dioxide (SO_2) and Carbonylsulphide (OCS), entering the stratosphere by troposphere-stratosphere-exchange processes (Holton et al., 1995; Fueglistaler et al., 2009), and by direct injections of volcanic material from modest to large volcanic eruptions (SPARC/ASAP, 2006; Bourassa et al., 2012). During times of low volcanic activity, the stratospheric aerosol load inevitably degrades towards a so called background state representing the lowest possible self-maintaining aerosol level in the stratosphere. However, this natural balance ~~is~~ may be influenced by sulphur releasing anthropogenic activities (Hofmann et al., 2009; Neely et al., 2013). Together with the sporadically occurring volcanic perturbations, human activities alter the Earth's radiative balance, in turn affecting the long-term trend of the global aerosol load (Solomon et al., 2011). The relative contributions of the precursors to maintain the background Junge layer as well as their major pathways into the stratosphere (apart from direct injections by volcanoes) are not well understood (e.g. Hofmann, 1990; Deshler et al., 2006; SPARC/ASAP, 2006; Hofmann et al., 2009; Bourassa et al., 2012; Brühl et al., 2012; Rex et al., 2012; Neely et al., 2013).

With respect to the much-debated potential to moderate climate change by manipulating the Earth's albedo due to the enhancement of the stratospheric aerosol load, e.g. the Royal Society Report on Geoengineering the Climate (Society, 2009) explicitly emphasised a considerable demand to better understanding the spatio-temporal variability of the stratospheric aerosol system, including the barely explored coupling between the dynamics of the upper troposphere and lower stratosphere (UT/LS) and microphysical processes which are ultimately determining load, size and stability of this system. ~~These problems are addressed in the current study.~~ Our study addresses in particular the latter issues as we will explain below.

A variety of fundamental questions of the stratospheric aerosol system have been addressed in the

review of stratospheric aerosol processes by the WMO/SPARC initiative (SPARC/ASAP, 2006). ~~It largely~~ **The report** focussed on conditions observed after the powerful eruption of Mt. Pinatubo in 1991, which significantly influenced both the stratosphere and the Earth's climate in the subsequent two to three years. SPARC/ASAP (2006) also revealed a few remarkable scientific issues related to stratospheric background conditions. For instance, the report emphasised that measured LS aerosol quantities distinctly differ between the observational systems (in-situ, remote). More recent studies addressed this problem in several ways (e.g. Thomason et al., 2008; Damadeo et al., 2013) but since the decommissioning of the ERBS satellite in 2005, which hosted the SAGE II instrument, equivalently well examined data sets of vertically-resolved stratospheric aerosol size properties do not exist.

Another major uncertainty of the stratospheric aerosol system arises from the lack of observations of the precursors SO_2 and H_2SO_4 vapour in the stratosphere. SO_2 and H_2SO_4 vapour quantities have not yet been systematically monitored in the LS - contrary to the troposphere, in particular the boundary layer. Only a few individual measurements of the two gases were conducted in the stratosphere during balloon ascents in the nineteen-seventies and -eighties (see Hommel et al., 2011, herein referred to as HOM11, for a review). Only a single remotely sensed SO_2 profile existed for altitudes above 30 km, obtained during a NASA Space Shuttle mission in 1986 (Rinsland et al., 1995), until very recently a new SO_2 data set has been derived from Envisat/MIPAS observations (Höpfner et al., 2013).

With respect to modelling initiatives aiming to better understand the stratospheric aerosol-climate system, there has also scarcely been any progress since SPARC/ASAP (2006) emphasised distinct differences between modelled aerosol quantities and observations. Most studies of global climate models with interactively coupled aerosol size and microphysics schemes focus on the examination of the tropospheric aerosol-climate system, predominately detached from stratospheric aerosol processes (Ghan and Schwartz, 2007; IPCC, 2013). Only a very limited number of studies addressed aerosol processes in the UT/LS by means of aerosol size resolving microphysics models that have been interactively coupled to global climate models. Some studies focussed on the determination of aerosol induced climate effects of the Mt. Pinatubo eruption 1991 ~~(Niemeier et al., 2009)~~ (Niemeier et al., 2009; English et al., 2013) Other studies investigated the stability of the Junge layer during the stratospheric background periods ~~(Timmreck, 2001; Pitari et al., 2002; Hommel et al., 2011; English et al., 2011; Brühl et al., 2012)~~ (Timmreck, 2001; Pitari et al., 20

~~In this study we address the coupling between the stratospheric dynamics and aerosol microphysical processes, whose understanding is key to evaluate stratospheric geoengineering options.~~ **In this study we address certain aspects of the coupling between stratospheric dynamics and aerosol microphysical processes, as they are important to understand the contributions of QBO and natural variability to recent observed changes of stratospheric aerosol, and as they are key to evaluate stratospheric geoengineering options.** We focus on effects imposed by the quasi-biennial oscillation (QBO) in the tropical stratosphere (reviewed in Baldwin et al., 2001) as this dominant

mode of stratospheric variability largely impacts the global dispersion of stratospheric trace constituents (e.g. Gray and Chipperfield, 1990). **In particular we address the QBO signatures in the aerosol mixing ratio, in the integral and resolved aerosol size as well as in the abundance of aerosol precursors. Furthermore, we estimate the QBO signal in microphysical processes determining the transfer of sulphur mass between the gas and aerosol phases, i.e. nucleation and condensation/evaporation.**

We elaborate a numerical experiment to simulate an 11–yr stratospheric background period after 1995, when the stratosphere had recovered from the violent eruption of Mt. Pinatubo in June 1991 (SPARC/ASAP, 2006). This is done by coupling an aerosol size resolving microphysics scheme (SAM2; HOM11) and a middle-atmosphere circulation model (MAECHAM5; Manzini et al., 2006) that precisely specifies the QBO (Giorgetta and Bengtsson, 1999). To avoid any interference with effects superimposed from other external sources, the model is driven in a climatological mean configuration and does not consider any volcanic or pyro-cumulonimbus injections into the stratosphere. The analysis ~~focus~~ focusses on the spatio-temporal evolution of the Junge layer in the tropics, because the QBO signature is strongest in the equatorial belt. Modelled aerosols do not radiatively feed back to the general circulation and the QBO, neither directly nor by impacting the stratospheric ozone chemistry. Both may be important in particular for the extra-tropics and are in the scope of following studies.

Although stratospheric aerosols have been monitored with sufficient global coverage since the end of the ~~seventies~~nineteen-seventies, QBO signatures in observed post-Pinatubo stratospheric background aerosol quantities have only been inferred in a very limited number of studies (Choi et al., 1998, 2002; Barnes and Hofmann, 2001). Since these studies do not show QBO signatures in other aerosol quantities than the retrieved extinction coefficients or the aerosol backscatter, in this study we also infer QBO signatures from climatologies of the aerosol surface area density ~~and the aerosol effective radius, both~~ inferred from SAGE II retrieved extinction coefficients, in order to establish a direct comparison between our modelled aerosol properties and observations. **In a consistent manner we also compare QBO signatures in SO_2 observed by MIPAS (Höpfner et al., 2013) with our simulation.**

We want to emphasise that the focus of our paper is the QBO-aerosol microphysics relationship and not an analysis of the stratospheric aerosol record as observed in the recent past. Other studies indicated the relevance of non-sulphate and mixed aerosols, for instance meteor debris (reviewed in Neely et al., 2011) , volatile organics (e.g. Froyd et al., 2009) or carbon (e.g. Murphy et al., 2007) , for the stratospheric aerosol burden, optical depth, and the radiative forcing. Here we focus on sulphate aerosols because they clearly dominate the stratospheric aerosol mass (see SPARC/ASAP, 2006) . An understanding of the mechanisms determining the variability of the main reservoir of stratospheric aerosol is mandatory in order to separate the signatures of atmospheric dynamics, microphysics and volcanoes from the observed LS aerosol record in future studies. In this

respect, our work can be seen as a necessary step towards an in-depth understanding of the lower stratospheric aerosol system by utilising a model system of reduced complexity.

The paper is structured as follows: First we give a brief overview about the model used in this study. The following sections describe the influence of the QBO on a variety of modelled aerosol ~~parameters in the equatorial stratosphere and compare the results to other data from observations or models.~~ parameters, size distributions and on the precursor gases $\mathbf{SO_2}$ and $\mathbf{H_2SO_4}$ in the equatorial stratosphere. Our results are compared with other data from observations and models. The final section summarises our findings.

2 Methodology

2.1 Model framework

The model framework used to assess the interannual variability of the aerosol layer in the tropical stratosphere during times of stratospheric background is identical to the model described in detail in HOM11. In this study a middle-atmosphere general circulation model with an interactive, particle size-resolved aerosol dynamics module was evaluated against satellite data and in-situ observations. The major difference between the companion study of HOM11 and this work is the representation of the quasi-biennial oscillation in the equatorial stratosphere. While our applied model setup has no internally generated QBO (Giorgetta et al., 2002, 2006), we perform an additional experiment in which the QBO is nudged towards observed winds from radiosonde measurements at Singapore (updated from Naujokat, 1986) by applying the method of Giorgetta and Bengtsson (1999). Hereafter, comparisons between the two model setups are referred to as CTL (control run) for the free running model of HOM11, and QBO for the QBO-nudged simulation. For details on the host model and the aerosol dynamics scheme we refer the reader to HOM11 - in the following only the basic features needed to understand the experimental set up are described.

The model was integrated in T42 truncation, using an associated grid with a horizontal resolution of about 2.8°x2.8°. In the vertical, 39 sigma-hybrid layers resolved the atmosphere up to 0.01 hPa ($\sim$ 80 km) with a layer thickness increasing from about 1.5 km to 2 km in the region of the tropical Junge layer. Around the stratopause, the layer thickness is about 3 km , further increasing towards the model's top of atmosphere to $\sim$ 6.5 km (Giorgetta et al., 2006, their Fig. 1). The time integration interval was 15 min. In the QBO configuration, the modelled zonal wind in the equatorial stratosphere is nudged towards the zonal wind profile observed at Singapore (see Giorgetta and Bengtsson, 1999), assuming a Gaussian latitudinal distribution of the zonal wind about the equator with a half width increasing from 7° at 70 hPa to 10° at 10 hPa. The nudging rate is 1/(10 days) between 70 hPa and 10 hPa and between 10°N and 10°S. Poleward of 10° latitude the nudging rate is linearly reduced to zero at 20° latitude. Outside of this region the zonal wind remains unaffected by the nudging scheme.

To ensure that the model's interannual variability is unaffected by the prescribed boundary conditions, we applied perpetual monthly climatologies of AMIP2 sea surface temperatures and sea ice concentrations as lower boundary conditions. Natural and anthropogenic sulphur emissions were taken from the AeroCom database (scenario B) and represent year 2000 conditions (Dentener et al., 2006).

In the microphysics scheme SAM2 (HOM11), aerosols are resolved throughout the atmosphere in 35 logarithmically spaced bins that range from 1 nm to 2.6 $\mu\mathrm{m}$ in radius. For the sake of computational efficiency aerosols are assumed to be composed of a binary $H_2O-H_2SO_4$ mixture, which is a reasonable assumption under stratospheric conditions (e.g. Hamill et al., 1997). Microphysical processes considered are binary homogeneous nucleation (BHN; Vehkamäki et al., 2002), condensation and evaporation of water and sulphuric acid, as well as Brownian coagulation and gravitational sedimentation. In the troposphere, aerosol washout processes and surface deposition are treated as in Stier et al. (2005). Aerosols are advected segment-wise employing a semi-Lagrangian advection scheme (Lin and Rood, 1996) in terms of their mixing ratio relative to the mass of sulphur (S) incorporated in the droplets.

~~Similar to HOM11, the model applies an offline chemistry scheme based on prescribed climatological monthly zonal mean oxidant fields of , , , . Also mixing ratios are prescribed.~~ **Similar to HOM11, the model applies an offline sulphur chemistry scheme, using prescribed monthly and zonal mean oxidant fields of OH, O_3, NO_2, H_2O_2 from a climatology of the MOZART2 CTM (Horowitz et al., 2003) . Similarly, OCS mixing ratios are prescribed based on a climatology from the MESSy CCM (Jöckel et al., 2005) .** The aerosol radiative effects follows the ECHAM5 standard approach and rely on emissivities obtained from the Tanre et al. climatology (see Roeckner et al., 2003). Interactions between aerosols and the cycles that form and maintain high altitude clouds (cirrus and polar stratospheric clouds) have not been considered.

The model was run over 17 years, from January 1990 to December 2006. Only the last 11 years were analysed (1996 - 2006). ~~Hommel (2008) showed that the model reaches a steady state of the stratospheric aerosol layer after six years. Then no further impact from the initialisation of the model was detectable for any of the aerosol parameters.~~ **The preceding 6 years of simulation are influenced by the spin up of the model from the aerosol initialisation. In a technical note, Hommel (2008) showed that the modelled aerosol layer reached a steady state within that time. As of year 6, no further impact from the initialisation was detectable for any of the diagnosed aerosol parameters.**

2.2 Observational aerosol data

For comparison, we use the aerosol ~~forcings data set~~ surface area density (SAD) dataset compiled for the WMO/SPARC Chemistry Climate Model Initiative ~~(CCMI;). This data set~~ (CCMI; http://www.pa.op.dlr.de/CCMI; Eyring et al., This dataset provides consistent aerosol forcings for the troposphere and stratosphere up to 39.5 km

($\sim$ 3 hPa). For the stratospheric background period between 1996 and 2006, this gridded and gap filled ~~data set~~ dataset combines observations from the satellite instruments ERBS/SAGE II (1996 - May 2005) and Calipso/CALIOP (June 2005 - December 2006). Aerosol surface area densities ~~(SAD)~~ were derived from SAGE II (~~vn7~~v7) size distribution fits to measured aerosol extinction coefficients in four ~~wave-lengths~~ wavelengths as described in Arfeuille et al. (2013). This method takes the composition of aerosol droplets (weight percentage) into account, as determined by stratospheric temperature and water content of the ECMWF ERA-Interim reanalysis. CALIOP SAD were obtained from a conversion of the measured aerosol backscatter into extinction coefficients at 532 nm ~~wave-length~~ wavelength and a subsequent fit of uni-modal log-normal distributions based on SAGE II extinction correlations (Beiping Luo, ETH, personal communication July 2013).

In relation to the SADs of the predecessor initiative CCMVal (Chemistry-Climate Model Validation Activity) forcing ~~data set~~ dataset (http://www.pa.op.dlr.de/CCMVal/Forcings/CCMVal_Forcings_WMO2010.html), the newer data provide a much better representation of aerosols in the post-Pinatubo stratospheric background period. Beyond 2004 CCMVal SADs were represented as recurring 5yr–averages from 1998 to 2002, that erase any information about the QBO-Junge layer relationship in the equatorial stratosphere from the data and largely impact the derivation of anomalies from the long-term average.

A comparison to other ~~data sets~~ datasets and gridded climatologies of aerosol size properties is not possible at this point, because those either cover a few years of the post-Pinatubo stratospheric background only (Bauman et al., 2003a,b; Wurl et al., 2010) or contain ~~to~~ too many gaps (SPARC/ASAP, 2006; Wurl et al., 2010), which makes a statistically meaningful calculation of residual anomalies impossible.

We also compare to the MIPAS SO_2 climatology of Höpfner et al. (2013) , providing a so far unprecedented record of near global observations of this aerosol precursor gas in the lower stratosphere. The time-series contains gridded (18 10-degree latitude bins between 85°N and 85°S, 36 level) monthly mean zonal means between 07/2002–04/2012, ranging in the vertical from 15 to 45 km. Here, we analysed data up to 40 km, and averaged meridionally between 5°N–5°S. For a meaningful comparison to our model, we interpolated MIPAS data to pressure levels according to the ICAO standard atmosphere. It shall be noted that the dataset contains about 17 % missing data (monthly mean zonal means on the analysed levels), which may affect the calculation of robust QBO signatures. All of the missing values appear before 10/2006, hence, overlap with the time-series from our model, ending in 12/2006. To provide statistically significant QBO signatures, we therefore decided to analyse the entire MIPAS time-series, even though the time frames do not coincide. It shall also be emphasised that the Höpfner et al. (2013) climatology inherently contains the signatures of direct volcanic injections and from volcanic material which is rapidly uplifted from the troposphere into the LS (discussed in Bourassa et al. (2012) , Vernier et al. (2011) , and Vernier et al. (2013)). Such

a volcanic influence on the Junge layer is, as mentioned above, not considered in our model simulation. For the sake of simplicity we refer the reader to Höpfner et al. (2013) , describing the retrieval method and discussing the quality of the retrieved SO_2 profiles in comparison to e.g. the ATMOS and ACE-FTS profilers. Höpfner et al. (2013) also provide a regression analysis to determine the different signatures of natural forcings.

2.3 Meteorology

The model's ability to adequately reproduce the QBO through the nudging procedure is assessed by comparison to the ECMWF ERA-Interim reanalysis. Fig. 1 compares the temporal development of the ERA-Interim zonal mean zonal wind at the equator from 1996 to 2006 (Fig. 1a) to the two model configurations (Fig. 1b,c). Through QBO-nudging the temporal behaviour of alternating zonal mean zonal winds in the model applied in this study is well reproduced (Fig. 1b), whereas in the free-running model (CTL) easterly winds prevail in the lower tropical stratosphere throughout the year (Fig. 1c). ~~Also the onset of the descent of the QBO above 10 is adequately reproduced in the nudged model, although in this region no nudging was performed.~~ **In the middle stratosphere, this easterly zonal wind regime is only being influenced by moderately strong westerlies (<10 $\mathrm{m\,s^{-1}}$) of the semi-annual oscillation (SAO) in the mesosphere and upper stratosphere. The westerlies are able to penetrate down to the 30 hPa pressure level. In the nudged model, also the onset of the descent of the QBO above 10 hPa is adequately reproduced, although in this region no nudging was performed.**

Fig. 2 shows associated temperature anomalies in the equatorial stratosphere that are imposed by the QBO to maintain the thermal wind balance. The QBO signature is expressed in this figure as a residual anomaly, composited relative to the time of wind shear onset at 18 hPa (reanalysis at 20 hPa). The reanalysis (Fig. 2a) is 3 to 4 K colder around 10 hPa during times of easterly shear and 2 K warmer during westerly shear between 50 and 30 hPa than the ~~QBO nudged~~ QBO-nudged model (Fig. 2b). The model shows somewhat stronger anomalies above 10 hPa. ~~As the climatologies of the equatorial zonal winds differ between the QBO and CTL experiments, also the temperature profiles differ (Fig. 2c). In the QBO simulation the QBO easterlies and westerlies dominate in the upper and lower stratosphere, respectively, thus create a time mean vertical shear that results in temperature anomaly profile that is negative in the middle stratosphere and positive above the tropopause and below the stratopause, compared to the case of the CTL simulation with very weak wind shear in the climatological mean.~~ **As the climatologies of the equatorial zonal winds differ between the QBO and CTL experiments, also the temperature profiles differ (Fig. 2c). In the QBO simulation the QBO easterlies and westerlies dominate in the upper and lower stratosphere. This causes a vertical shear in the time-mean that results in $\sim$1 K lower temperatures in the middle stratosphere and 1–2 $\sim$1 K higher temperatures above the tropopause and below the stratopause, compared to the CTL simulation with a very weak wind**

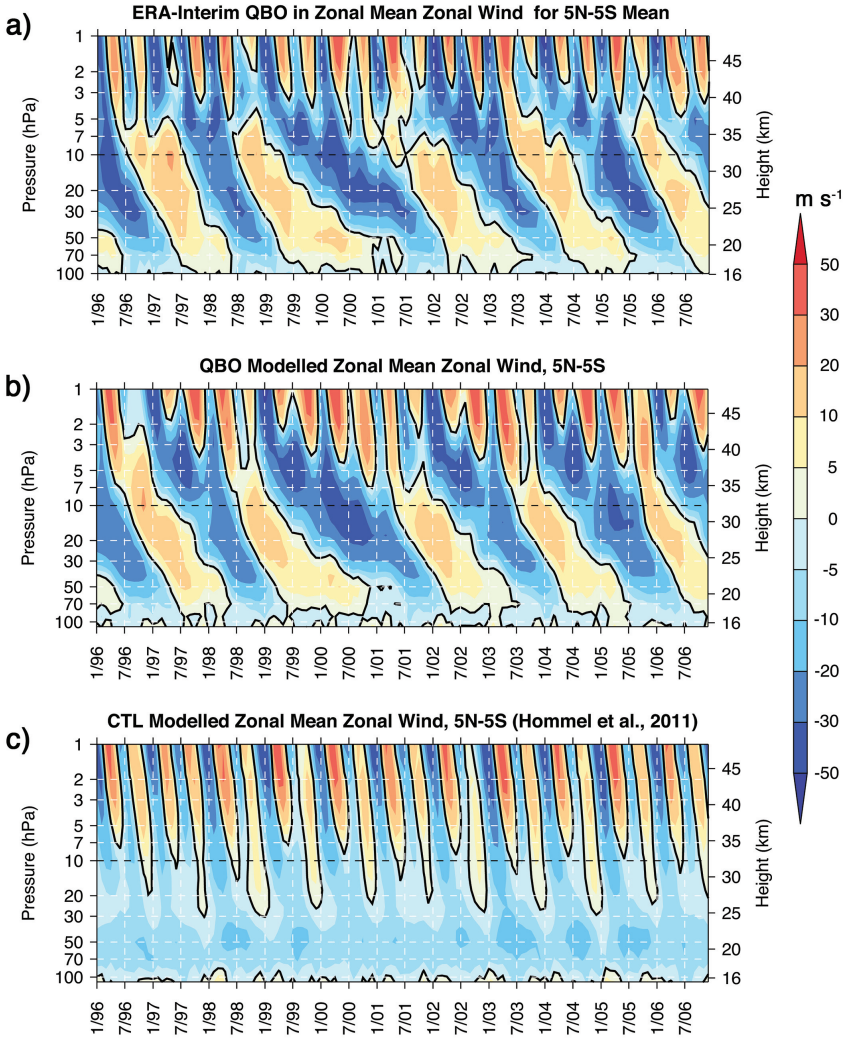

Fig. 1. Temporal evolution of the monthly zonal mean zonal wind in the equatorial lower stratosphere between 5°N and 5°S for the years 1996–2006 in the (a) ECMWF ERA-Interim reanalysis and MAECHAM5-SAM2 simulations (b) with QBO-nudging and (c) in the control experiment (CTL) of Hommel et al. (2011). Reddish colours represent westerlies, blueish easterlies. Black countours highlights the month and altitude of wind transition.

shear in the climatological mean. Thus, in the time mean the CTL simulation has colder tropical tropopause layer (TTL) conditions than the more realistic QBO simulation with an imposed QBO. This also affects the mean tropical upwelling that is reduced by approximately one half between 70 hPa and 50 hPa in the nudged model, and improves the representation of the water vapour tape recorder (Giorgetta et al., 2006).

From Fig. 1 it is obvious that only the model which represents the QBO realistically describes the

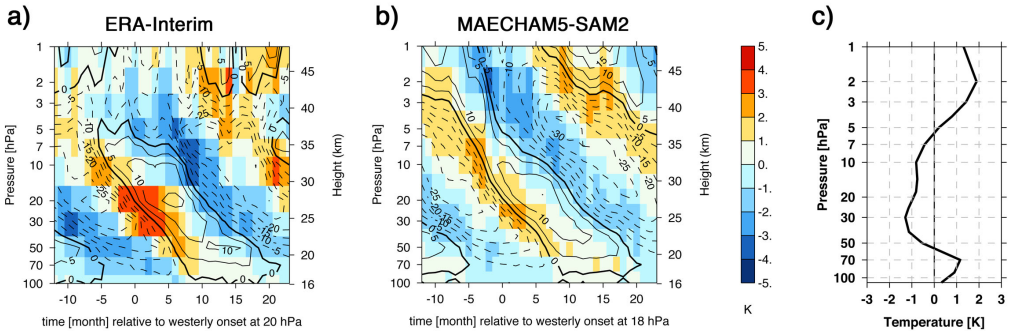

Fig. 2. Residual temperature anomalies induced by the QBO in (a) the ERA-Interim reanalysis and (b) the QBO-nudged MAECHAM5-SAM2 simulation between 5°N and 5°S. Composited for the years 1996–2006 relative to the onset of residual westerlies at 20 hPa and 18 hPa, respectively. Black contours denote the residual zonal mean zonal wind, where dashed lines represent easterlies. Contour interval is 5 $\mathrm{m\,s^{-1}}$. The difference between the climatological averaged temperature profiles of the QBO-nudged simulation and the control experiment (QBO-CTL) is shown in (c).

variability in the equatorial stratosphere. This may have implications for thermodynamic properties of aerosols in this region and for the processes that form and maintain the aerosol layer.

3 Results and Discussion

Observational evidence that the QBO affects the stratospheric aerosol layer came from aerosol extinctions measurements in the early years of systematically monitoring the stratosphere from space (e.g. Trepte and Hitchman, 1992; Grant et al., 1996). In an aerosol-coupled chemistry climate model simulation, Brühl et al. (2012) reproduced the temporal development of the tropical aerosol mixing ratio that has been inferred from SAGE II extinction measurements. But their time-slice experiment was conducted for 33 months during a period of low volcanic activity in the stratosphere between January 1999 and September 2002, that only covers a single QBO cycle. In the following, the influence of the QBO on the modelled aerosol mixing ratio is examined and their influence on other parameters describing the aerosol population in the stratosphere are investigated. Conclusively, QBO signals in precursors are examined and implications for aerosol formation and growth are given.

3.1 Aerosol mixing ratio

3.1.1 Temporal evolution

The configuration of the model in HOM11 did not allow to consider QBO effects on stratospheric trace constituents. Therefore, in the HOM11 study, the Junge layer behaves almost statically, in the

tropics only being influenced by temperature variations in the TTL and wind alterations related to the semi-annual oscillation (SAO) in the mesosphere and upper stratosphere (Fig. 3a; see also Giorgetta et al., 2006). Fig. 3b shows the strong variability in the temporal evolution of the modelled aerosol mixing ratio in the equatorial lower stratosphere of the ~~QBO nudged~~ QBO-nudged experiment.

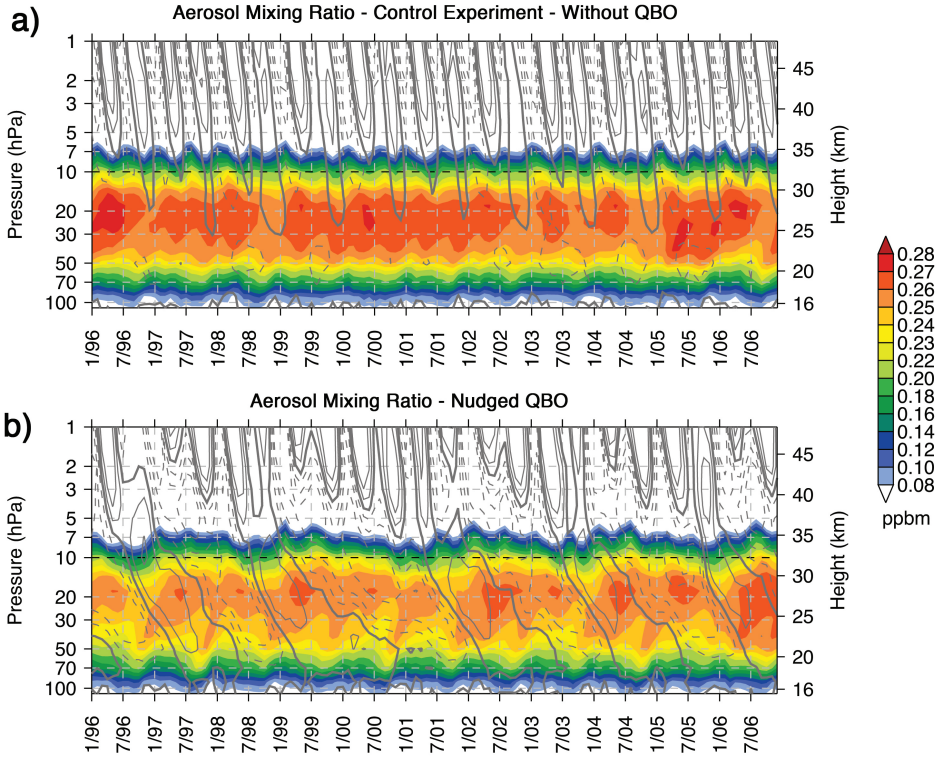

Fig. 3. Temporal evolution of the monthly mean zonal mean aerosol mass mixing ratio ($\mathrm{x10^9\ kg(S)/kg}$) in (a) the CTL simulation of Hommel et al. (2011) and (b) the QBO-nudged model between 5°N and 5°S for the years 1996–2006. Gray contours denote the zonal wind as in Fig. 1, where dashed lines represent easterlies.

Without a QBO, anomalies in the aerosol mixing ratio, relative to the climatological mean annual cycle, appear like the tape recorder signal (not shown) in tropical stratospheric water vapour (Mote et al., 1996). ~~In contrast~~ **Zonal winds of the SAO modulate the maximum vertical extent of the layer by 1–3 km, but do not interfere much with the annual cycle below ~14 hPa. The layer is thicker in the SAO easterly shear - the mechanisms are the same as for the QBO, and are discussed in the following.**

In contrast to the CTL simulation, the interannual variability of the tropical aerosol layer in the QBO-nudged experiment is much stronger and depends on the strength and direction of the zonal winds in the equatorial stratosphere. The QBO directly influences the vertical extent of the layer and modulates the peak aerosol mixing ratio in the tropical stratospheric reservoir (TSR; Trepte and Hitchman, 1992) by about 5 %, relative to the CTL simulation, with larger values seen during

times of maximum easterly wind acceleration. The difference in the variability of the modelled aerosol mixing ratio at the equator is also expressed in the profiles of the inferred peak-to-peak amplitudes of the annual cycles and the QBO (Fig. 4). In the upper tail of the aerosol layer, i.e. around 10 hPa, the annual cycle is approximately one third weaker in the QBO-nudged simulation than in the model without a QBO. In contrast, the seasonality in the lower regions of the aerosol layer is approximately 25 % stronger in the QBO-nudged model due to the more realistic upwelling above the TTL (Giorgetta et al., 2006) . The weaker seasonality around the upper tail of the layer results from the much weaker interference of the SAO with the lower stratosphere in the QBO-nudged simulation, as described above.

The peak-to-peak amplitude of the QBO maximises at the 7 hPa pressure level and is there about twice as strong as the annual oscillation at 10 hPa. Between 70 and 14 hPa, where the largest aerosol mixing ratio is found both modulations are relatively week, compared to their magnitudes around the lower and the upper tail of the layer. Between 70 and $\sim$ 30 hPa the amplitude of the QBO is up to twice as strong as the annual cycle, suggesting larger aerosol dynamical effects in the region than in the CTL simulation, as we will discuss in the following.

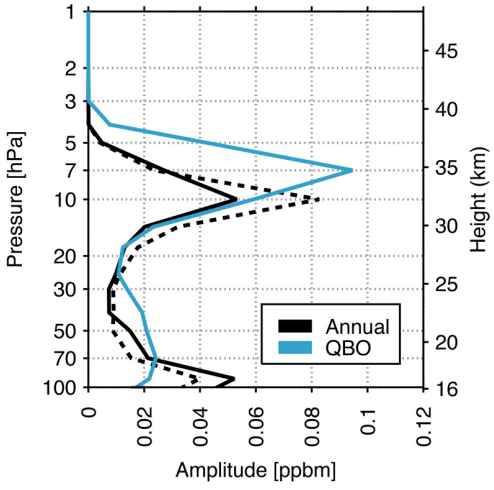

Fig. 4. Comparison of the approximate peak-to-peak amplitudes of the annual cycle and the QBO in the simulated aerosol mixing ratio o

The characteristic patterns of upward and downward motion of the tropical Junge layer that have been inferred from the time-series of equatorial aerosol mixing ratios in the QBO-nudged simulation (Fig. 3b) result from a superposition of advection by the ~~extra-topically~~ extra-tropically driven Brewer-Dobson circulation (BDC), the meridional circulation imposed by the QBO (also known as the secondary meridional circulation, SMC, or residual circulation of the QBO), and the annual cycle in the tropopause temperature ~~.~~ (see the reviews of e.g. Holton et al. (1995) ,

Baldwin et al. (2001) , and Fueglistaler et al. (2009)). The thermal wind relationship requires that westerly zonal wind shear is balanced by warm anomalies . (e.g. Andrews et al., 1987) . This causes a descent of equatorial air relative to the tropical upwelling that is associated with the BDC. Consequently, easterly zonal wind shear is balanced by cold anomalies and induced relative ascent. The associated meridional circulation is characterised by anti-correlated upward (downward) motion in the extra-tropics at levels of QBO westerly (easterly) shear, and meridional convergence (divergence) in the QBO westerly (easterly) jet. Hence, advective effects of the secondary circulation of the QBO on the QBO jets contributes to narrower (in latitude) and deeper westerly jets compared to wider and shallower easterly jets. Due to this secondary circulation also the tropical reservoir that is confined by the sub-tropical mixing-barrier (e.g. Grant et al., 1996) expands meridionally (horizontal divergence) during the time of maximum easterly zonal wind acceleration and appears compacted in the vertical (vertical convergence). The secondary circulation determines the meridional extent of the TSR which is confined by the sub-tropical mixing-barriers (e.g. Trepte and Hitchman, 1992; Grant et During the time of maximum easterly zonal wind acceleration it expands meridionally (horizontal divergence) and appears compacted in the vertical (vertical convergence). The opposite is the case during times of maximum westerly zonal wind acceleration: The tropical stratosphere is narrowed in the horizontal and stretched in the vertical. Those structures are easily inferable from concentration gradients of stratospheric trace constituents. A respective model goes back to the works of Plumb and Bell (1982), for TSR aerosol it was first reported by Trepte and Hitchman (1992) based on aerosol extinction measurements from SAGE I and II instruments in the periods 1979-81 and 1984-91, when the volcanic aerosol load of the stratosphere was relatively low. Underlying mechanisms were later examined in detail by Choi et al. (1998) and Choi et al. (2002) from HALOE observations of aerosol extinction, ozone and other trace gases.

These relationships are responsible for the characteristic temporal evolution of the simulated Junge layer in the tropics: As seen in Fig. 3b, the largest vertical expansion of the Junge layer slightly lags behind the occurrence of strongest QBO westerlies at 30 - 20 . And the largest reduction in the vertical extent is found after QBO easterlies were strongest above 20 . This vertical spread of the layer is accompanied with an increase in its top height, that varies from around 10 during times of the onset of westerly winds and $\sim$ 6 in the aftermath of the easterly QBO shear. This increase in top height is more distinct at lower altitudes where the layer is denser, i.e. between 20 and 10 . For instance, in this region the 0.35 mixing ratio isopleth steeply raises vertically after westerlies were strongest. A large lofting of particulate material is also found in the lower regions of the layer, that, moreover, outweigh displacements at its top edge. Bottom displacements are in the order of 3 - 5 , whereas the layer's top drifts no more than 2-3 km. . To better illustrate the net-effect of the QBO on the simulated aerosol mixing ratio (Fig. 5a) we have composited the time-series (Fig. 3b) similarly to the temperature anomaly composites (Fig. 3), i.e. relative to the onset of the westerly zonal wind shear at 18 hPa. The corresponding deviation in geometric altitude

of the 0.25 ppbm isopleths is shown in Fig. 5b as well as the approximated thickness of the Junge layer, expressed as vertical extent between the 0.25 ppbm isopleths above and below the modelled maximum aerosol mixing ratio.

~~It is nicely seen in Fig. 3b~~

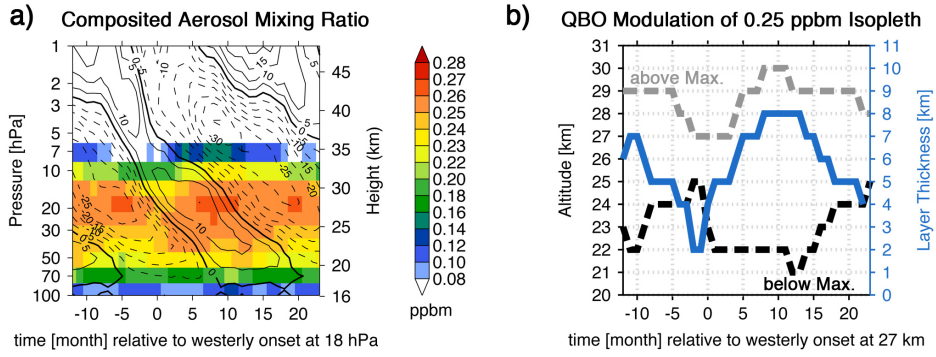

Fig. 5. (a) Composite of the simulated aerosol mixing ratio in the QBO-nudged model relative to the onset of residual westerlies at 18 hP

As seen in Fig. 5, and Fig. 3b, the largest vertical expansion of the Junge layer slightly lags behind the occurrence of strongest QBO westerlies, when the layer thickness can reach 8 km. The largest reduction in the vertical extent lags behind strongest QBO easterlies and reaches 2 km at minimum. The vertical spread of the layer is accompanied with an increase in its top height (expressed by mixing ratios < 0.08 ppbm), varying between ~ 10 hPa during times of the onset of westerly winds and ~ 6 hPa in the aftermath of the easterly QBO shear (note, that the 0.25 ppbm isopleth of Fig. 5b is distinctly below the layer's upper lid). In contrast to the composite plots, where local effects may be smeared by the somewhat irregular period of the QBO, from the time-series of Fig. 3b one can better infer that the increase in the layer's top height is stronger at lower altitudes where the layer is denser, i.e. between 20 and 10 hPa. For instance, the gradient of the 0.25 ppbm isopleth above the mixing ratio maximum is steeper after the strongest QBO westerlies. In the composites, however, this gradient appears smoother. In the lower regions of the layer the lofting of aerosols outweigh displacements at its upper lid. Bottom displacements are in the order of 3–5 km, whereas the layer's top drifts no more than 2–3 km.

It is clearly shown in both the time-series (Fig. 3b) and the composite (Fig. 5a) that after the layer reaches its largest vertical expansion, the model predicts that the entire layer descends under the influence of descending easterly zonal winds. As mentioned above, this descent is in the order of ~~2 - 3~~ 2–3 km around the onset of the westerly wind shear around the 15 hPa pressure level. This settling is accompanied by the above mentioned horizontal divergence of the TSR, which shifts the

subtropical mixing barriers a few degrees poleward (Grant et al., 1996; Neu et al., 2003). The net change of this variation, that is the difference in the layer thickness due to the QBO, is at least 5 km **(Fig. 5b)**.

Since this spatio-temporal structure of TSR aerosols is intrinsically linked to circulation patterns superimposed by the QBO in the tropical upwelling branch of the BDC, the model predicts that the SMC stabilise the Junge layer at higher altitudes, where in the QBO-free model of HOM11 aerosols are no longer thermodynamically stable. Mechanisms that act in particular on the top lid of the layer are discussed in greater detail in Sec. 3.4.

3.1.2 QBO induces anomalies in the tropical mixing ratio

To gain further insight into QBO effects on the dynamics of aerosols in the tropical lower stratosphere, in the following ~~(Fig. 6 - ??),~~ we discuss simulated anomalies induced by the QBO in aerosol mixing ratio and other LS aerosol properties. All data are zonal means and have been averaged between 5°N and 5°S. Profile data are climatological means of the analysed period. Composites of residual QBO anomalies, relative to the time of the onset of westerly zonal mean zonal wind at 18 hPa, were obtained from monthly means.

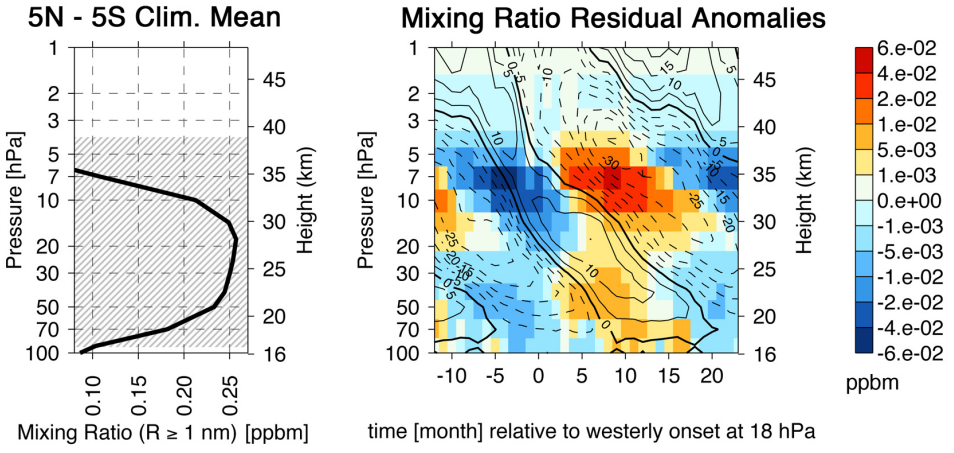

Fig. 6. (a) Climatological mean profile of the modelled aerosol mass mixing ratio between 5°N and 5°S for the period 1996–2006. (b) composite of ~~QBO induced~~ QBO-induced residual anomalies in the modelled aerosol mass mixing ratio with respect to the time of onset of westerly zonal mean zonal wind at 18 hPa. As in Fig. 2b, black contours denote the residual zonal wind. Dashed lines represent easterlies, contour interval is 5 $\mathrm{m\,s^{-1}}$. **Gray shades in (a) denote levels where the QBO signal exceeds the 95 % significance level, according to the standard Student's t-test.**

Fig. 6a shows the climatological averaged aerosol mixing ratio profile~~. Respective residual anomalies induced by the QBO are shown in Fig. 6b. Largest modulations are found in the regions~~

~~of large vertical gradients, especially in the upper levels near 7 to 10 , where sulphate droplets evaporate. During QBO east phase,~~ **, which is the time-average of the modelled temporal evolution of the equatorial aerosol mixing ratio (Fig. 3). The corresponding residual anomalies, induced by the QBO, are shown in Fig. 6b. The QBO signal is significant on the 95% confidence level (according to the Student's t-test) at all pressure levels where the mixing ratio exceeds 0.1 hPa. At the upper lid of the Junge layer, also QBO modulations of mixing ratios < 0.08 ppbm are significant.**

The QBO induces the largest anomalies where the vertical gradient in the mixing ratio is strong (Fig. 6b). Hence, strongest anomalies are found in the region where sulphate droplets evaporate, that is at the upper lid of the Junge layer, between 10 and 7 hPa. During QBO easterly phase, the bulk mixing ratio increases in this region by about 60 %. In the QBO westerly shear and during the QBO westerly phase a decrease relative to the mean annual cycle of 60 - 90 % is found. In contrast, around 20 hPa, where the bulk mixing ratio is largest, and below, in regions where the mixing ratio gradient is positive, only very moderate QBO modulations of less than $\pm$ 5 % are found.

~~A phase reversal in the sign of the anomalies is seen along the isopleths of descending zonal mean zonal winds around the 20 pressure level, where the aerosol mixing ratio is largest. Very similar anomalies are induced by the QBO in tropical stratospheric ozone. Ozone anomalies show a phase reversal around 10 that corresponds to the altitude of maximum ozone mixing ratio in the equatorial stratosphere (Hasebe, 1994; Butchart et al., 2003) . This~~ **A similar QBO signature has been found in the literature for tropical stratospheric ozone (see review in Baldwin et al., 2001) . From observations and models it is known that QBO induced ozone anomalies have phase reversals around 10 hPa, corresponding to the altitude of maximum ozone mixing ratio in the equatorial stratosphere (Hasebe, 1994; Butchart et al., 2003) .** The phase reversal results from QBO modulations in the vertical advection as discussed above. ~~Negative anomalies are produced in the westerly shear, where the vertical mixing ratio gradient is negative above 20 , and positive anomalies where the gradient is positive below 20 (Choi et al., 2002) .~~

QBO anomalies in our modelled aerosol mixing ratio exhibit such a phase reversal along isopleths of descending zonal mean zonal winds around the 20 hPa pressure level. This is the level where the aerosol mixing ratio is largest. Negative anomalies occur in the westerly shear, where the vertical mixing ratio gradient is negative (above 20 hPa), and positive anomalies where the gradient is positive (below 20 hPa). Ozone anomalies at the equator are reported to be in the order of 3 to 15 % (e.g. Butchart et al., 2003), hence are of similar strength as the QBO related aerosol variability in regions where the mixing ratio gradient is positive~~(below 20)~~. Above, in the evaporation region, the aerosol QBO is quite stronger with relative modulations ~~that exceed~~ exceeding 50 %. This implies ~~that~~ QBO modulations in the aerosol transport alone cannot explain this behaviour. Therefore, it is reasonable to assume that QBO modulates microphysical processes

as well, in particular the process of aerosol evaporation in higher altitudes (Sec. 3.4).

Despite the similarities between the QBOs in ozone and aerosol in the tropical lower stratosphere, there is a distinct difference between them: The thermodynamic limitation of the stability of liquid-phase aerosols in the LS imposes a characteristic oscillating temporal behaviour on the upper edge of the tropical Junge layer ~~(nicely seen~~ **(clearly shown** in the mixing ratio time-series Fig. 3b), which is not known from the ozone layer in the tropical stratosphere. Implications for the size of aerosols and processes that maintain them are discussed in the following sections.

3.2 Integrated aerosol size parameters

3.2.1 Surface area density

Integrated aerosol parameters ~~,~~ inferred from observed aerosol extinction coefficients at specific ~~wave length,~~ wavelength are fraught with uncertainties when the fraction of small particles significantly contributes to an aerosol size distribution (Dubovik et al., 2000; Thomason et al., 2008). ~~In particular, this becomes important when the aerosol load of the stratosphere is low (SPARC/ASAP, 2006) . HOM11 showed that integrated aerosol parameters of the CTL simulation vary considerably if the aerosol distribution is determined by condensational growth. It is therefore important to take this into account when modelled aerosol sizes are compared with observed data.~~ **SPARC/ASAP (2006) emphasised that this effect is particularly relevant when the aerosol load of the stratosphere is low. HOM11 showed that a systematic bias between observations and the CTL simulation arises in integrated aerosol size quantities when H_2SO_4 condensation dominates the growth of LS aerosols. Thus, in comparisons between integrated aerosol size quantities from models and remote sensing, particular attention should be paid to the systematic bias that is due to the fine mode fraction of aerosol populations.**

~~The SAD from the model simulation strongly depends on the size-range of the integration (Fig. 7a, c). The climatological mean SAD profile decreases with height, which results from persistent changes in the size spectrum of the particles: At lower levels, larger particles are more abundant than in the upper layers. This has two reasons: First, when particles grow, they are also removed quicker. A similar effect occurs when particles of a given size are advected into higher altitudes because their sedimentation velocity increases with height. Secondly, at higher altitudes the saturation vapour pressure of at the surface of the aerosol droplet increases so that the particles also evaporate quicker. Whereby larger aerosol particles evaporate at higher rates than smaller particles. Hence, with increasing altitude the size distribution of a stratospheric aerosol population is always shifted towards the fine mode.~~ **Also in our simulation, the SAD depends on the size-range of the integration. This can be seen by comparing the climatological mean profiles (Fig. 7a, c). When aerosols smaller 50 nm are not taken into account to mimic a satellite-sensor (panel c), the profile has a positive gradient below 70 hPa. It shows 10 % lower values at this particular pressure level,**

relative to the profile taking all simulated aerosol sizes into account (panel a). Above 70 hPa, both profiles decrease with height, which results from persistent changes in the size spectrum of the particles: At lower levels, larger particles are more abundant than in the upper layers. This is because the sedimentation velocity increases with height and at higher altitudes, the saturation vapour pressure of H_2SO_4 at the surface of an aerosol droplet increases so that the particles evaporate quicker. Both mechanisms shape the size distribution at higher altitudes towards the fine mode.

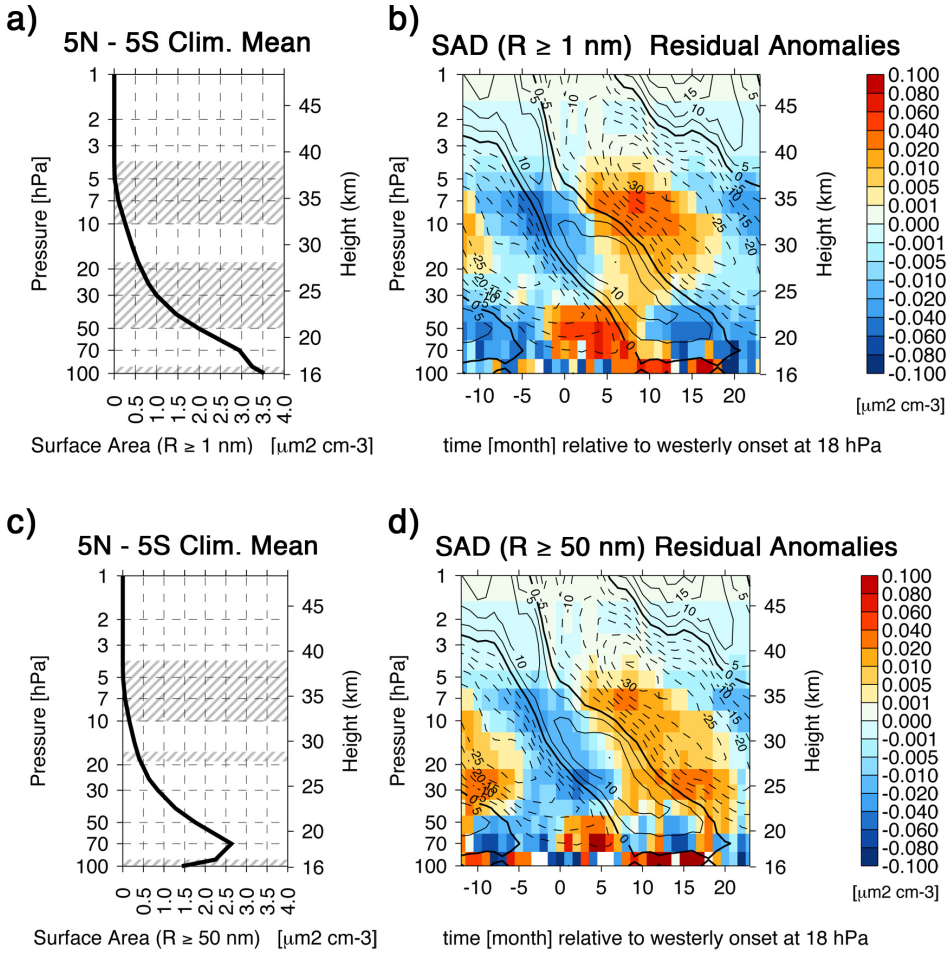

Fig. 7. As in Fig. 6, except for residual anomalies in the modelled aerosol surface area density (SAD). ~~Upper panel inferred from the entire size distribution $1\,\mathrm{nm} \leq R < 2.6\,\mu\mathrm{m}$, lower panel for aerosols with $R \geq 50\,\mathrm{nm}$.~~ **Data in the upper panels have been inferred from the entire modelled size distribution ($1\,\mathrm{nm} \leq R < 2.6\,\mu\mathrm{m}$). In the lower panels the aerosol size range has been adapted to the detectability of space-born remote sensors ($50\,\mathrm{nm} \leq R < 2.6\,\mu\mathrm{m}$).**

~~Compared to the CTL simulation, with a more or less static tropical Junge layer, the QBO nudged~~ **Compared to the CTL simulation (HOM11), with a less variable tropical Junge layer,** the QBO-nudged version shows 6 % lower SADs throughout the year between 80 hPa and 20 hPa. In contrast, directly above the TTL SADs are larger by 4 - 6 % in the QBO model and up to 30 % larger above the 10 hPa pressure level~~, where evaporation is strong.~~ . **This is the region where evaporation is strong.**

~~The climatological mean SAD (Fig. 7c) has a distinct different shape than the integral of the entire size spectrum (Fig. 7a), if one considers only aerosol sizes that are detectable by satellite-sensors (particle radii $<$ 0.005). The SAD increases from the TTL to 70 , where its maximum value is around 15 smaller. Here, the modelled aerosol spectrum is dominated by small, newly formed aerosols (HOM11), which would not be seen by the satellite-sensor. The effect on the QBO modulations inferred from the SAD integrals is shown in Fig. 7b and d. QBO anomalies themselves as well as their phase transitions between the lower and upper parts of the Junge layer are more pronounced in the SAD inferred from the entire aerosol spectrum. The relative strength of the QBO effects in the two SAD integrals, however, does not differ much below the 20 hPa pressure level and is in the order of $\pm$ 5 , relative to the absolute value.~~ **QBO signatures of the two SAD integrals also differ (Fig. 7b and d). In particular below 20 hPa, where the effect of the smaller aerosol arises which would not be seen by the satellite-sensor. Although the anomaly pattern are different, their relative strength is in the order of $\pm$ 5 % in both cases. Considering small aerosols in the calculation of the SAD increases the statistical significance of the inferred anomalies between 50–30 hPa. This also points to the important role of smaller particles for the SAD determination.**

~~This is different in the upper levels of the Junge layer: Above 20 relative SAD QBO modulations may exceed $\pm$100 %, although absolute values here~~ **Relative QBO modulations of the SAD are much stronger above 20 hPa. They may exceed $\pm$100 % although absolute values in this region** are more than one order of magnitude smaller than in regions of the layer further below. Those large modulations can be explained by QBO modulations in the reversible mass transfer of sulphuric acid vapour. In regions where warm (cold) anomalies are induced by the QBO in westerly (easterly) shear, the QBO fosters evaporation (condensation) and the SAD will be smaller (larger). In Sec. 3.4 we examine this relationship in more detail. ~~Also here in the evaporation region, there is almost no difference deducible in the relative strength of the modulations between the two SAD integrals.~~ **Similar to the region below 20 hPa, here the relative strength of the QBO modulations is approximately similar in the two SAD integrals.**

In contrast to the mixing ratio, statistical significance is limited to certain regions of the modeled SAD. The change in SAD from all sizes is significant at the 95 % confidence level, according to Student's t test, between 50–18 hPa and 10–4 hPa, and directly above the TTL below the 90 hPa pressure level. QBO related anomalies of the $\geq$50 nm SAD are significant

only where aerosols evaporate, i.e. 20–18 hPa and 10–4 hPa.

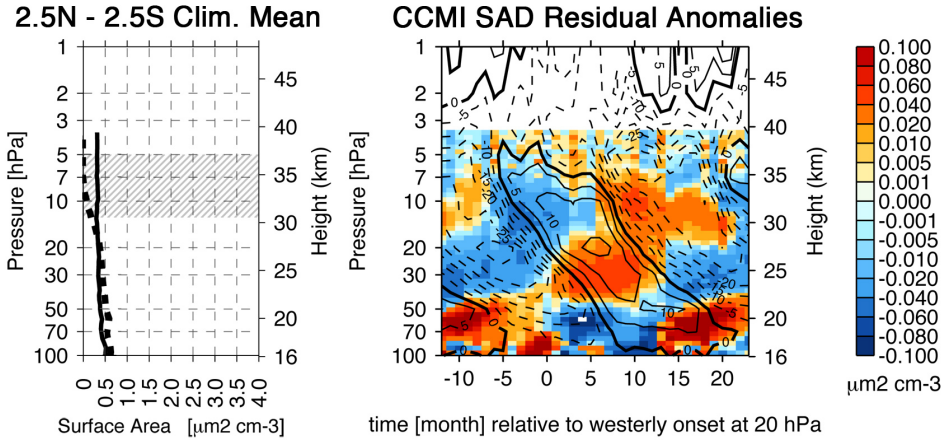

Fig. 8. As in Fig. 6, except for the SAD climatology between 2.5°N and 2.5°S of the SPARC CCMI initiative, inferred from spaceborne SAGE II and CALIOP observations. The profile in (a) is complemented by the climatological averaged SAD of the SPARC CCMVal initiative. The overlaid zonal wind in (b) is obtained from the ECMWF ERA-Interim climatology as in Fig. 2a.

The climatological mean surface area density profiles derived from satellite observations ~~is~~ are substantially smaller compared to the model ~~as shown in Fig. 8a for the two SAD data sets compiled for the WMO/SPARC initiatives CCMI and CCMVal as prescribed forcings for CCMs. Both data sets are based on SAGE II aerosol extinction observations (vn7 and vn6.2 of the operational NASA retrieval). HOM11 found a similar difference to SAGE II climatologies in a comparison of the modelled SAD of the CTL configuration with the retrieved SAD climatologies of Bauman et al. (2003a,b) and Wurl et al. (2010) . This agrees furthermore with SPARC/ASAP (2006) , that revealed a significantly positively biased SAD (factor 2 to 10) in the tropical LS for the majority of models that participated in an intercomparison, compared to the operational vn6.2 SAGE II SAD.~~ **as shown in Fig. 8a (below 20 hPa relative differences exceed factor 2). The datasets have been provided by the WMO/SPARC initiatives CCMI and CCMVal for the use in CCMs. HOM11 found similar differences between the modelled SAD of the CTL configuration and SAGE II SAD climatologies from Bauman et al. (2003a,b) and Wurl et al. (2010) . HOM11 emphasize that their comparison is in agreement with SPARC/ASAP (2006) , pointing out significantly positively biased SADs (by factor 2–10) in the tropical LS for the majority of models that participated in an intercomparison against the SAGE II v6.2 SAD.**

Below the 30 hPa pressure level, the climatological mean tropical profile of the CCMI SAD forcing data set is about 30 % smaller than in the CCMVal SAD forcing data set. Above ∼15 hPa the CCMI SAD forcing is distinctly larger with values above 0.3 $\mu m^2 cm^{-3}$, whereas, in contrast, the CCMVal SAD forcing tend to be zero. The latter indeed agrees better to our QBO and CTL

simulations, where above 15 hPa the aerosols begin to evaporate and ~~substantially~~ shrink in size, which imposes a net loss in mass and also in the aerosol's number density.

Although the climatological mean values of the CCMI SAD forcing data set at the equator are smaller than in our model simulations, observed ~~QBO induced~~ QBO-induced anomalies (Fig. 8b) ~~agree to a certain extent with our model predictions. Generally, the amplitudes of the inferred anomalies are similar, although they are slightly larger in CCMI between the TTL and about 40 hPa. The largest differences are found in the regions where the QBO westerly zonal wind is strongest between 50 and 20 . In contrast, above 20 QBO anomalies are in good agreement. It is likely that most of the somewhat irregularly appearing anomalies in the CCMI forcing data set below the 40 hPa pressure level reflect the release of volcanic material into the lower tropical stratosphere.~~ **agree to a certain extent with our model predictions, in particular above 20 hPa during the QBO east phase. Between the TTL and 20 hPa inferred anomalies are up to 60 % larger than in the model. This is very clearly reflected at pressure levels, where the QBO westerly zonal wind is strongest, i.e. between 40 and 20 hPa. Below 40 hPa, anomalies of opposite sign are found in CCMI compared to the model, in particular where westerly zonal winds prevail. This may reflect the release of volcanic material into the lower tropical stratosphere, which is not considered in the simulations.** Several moderate volcanic eruptions occurred in the later years of the analysed period (tropical volcano eruptions of Ruang occurred in late 2002, Manam in 01/2005, Soufriere Hills in 05/2006 and Tavurvur in 10/2006) and are suspected to have dispensed sufficient amounts of precursors in the tropical LS, that quickly formed new aerosols (Vernier et al., 2011; Neely et al., 2013). **The subsequent formation, dispersion and lofting of volcanic aerosol may have an effect on the inferred QBO signatures from CCMI. This relationship is complex, and needs further investigation, also taking other observations and data sets, as well as more specific model simulations into account.**

Inferred QBO signatures in the CCMI SAD are statistically significant at the 95 % confidence level between 14–5 hPa only. This is approximately the same altitude range where the R $\geq$50 nm SAD integral of the simulation is significant. Note, that in contrast to the simulation, where we used the t-test, for observational datasets (CCMI and MIPAS) we employed the F-statistics to compare the amplitude of the QBO spectral peaks to the red noise spectrum (e.g. Gilman et al., 1963; von Storch and Zwiers,

3.2.2 Effective radius

The aerosol effective radius (R_{eff}) is another key parameter widely used in the determination of UTLS aerosol climate effects (e.g. Grainger et al., 1995). Although negatively biased to ~~observations,~~ **the SAGE II climatologies of Bauman et al. (2003a,b) and Wurl et al. (2010) as well as in-situ observations of the balloon-borne optical particle counter of the University Of Wyoming (Deshler et al., 2003) ,** in the control experiment without a QBO, the model predicted R_{eff} lies within the uncertainty range

of the measurements (HOM11). Compared to the CTL experiment, the climatological mean tropical R_{eff} profile in the QBO experiment (Fig. 9a) shows 1 - 2.5 % smaller values, except in the lowest regions, between the TTL and 70 hPa, where it is about 2 % larger.

In Fig. 9b ~~QBO induced~~ QBO-induced R_{eff} anomalies are shown for aerosols larger than 50 nm in radius to ensure comparability with the particle sizes seen by remote sensing instruments. Although the patterns of QBO anomalies indicate strong modulations in R_{eff} except in the region between 20 - 10 hPa, their relative strength is ~~significant~~ **large** only above 10 hPa, where the size of evaporating aerosols rapidly decreases with increasing altitude. ~~Here, QBO related anomalies reach 60and are rather in-phase with anomalies in the mixing-ratio (Fig. 6b) than with anomalies in the SAD (Fig. 7b). Below 20 , QBO induced modulations are smaller than ± 5 , which is weaker than in the SAD.~~ **Here, QBO related anomalies reach 60 % and are approximately in-phase with anomalies in the mixing-ratio (Fig. 6b) and anomalies in the SAD (Fig. 7b). Below 20 hPa, QBO-induced modulations are smaller than ± 5 %, which is weaker than in the SAD. Statistical significance at the 95 % confidence level is reached throughout the equatorial belt, except between 10–4 hPa.**

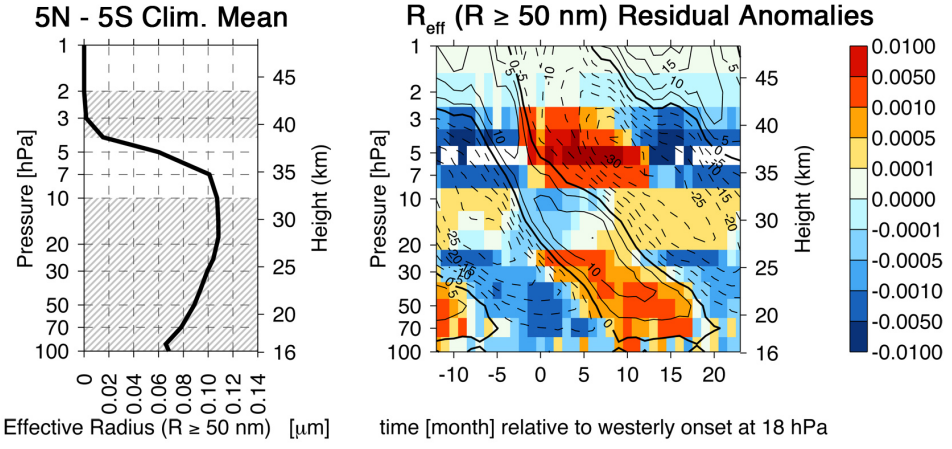

Fig. 9. As in Fig. 6, except for the modelled effective radius of aerosols with $R \geq 50\,\mathrm{nm}$.

No QBO signature would be seen in R_{eff} if the QBO affects the aerosol volume distribution and surface distribution in an equal measure. This is quite interesting in so far as HOM11 pointed out that most of the differences between the model R_{eff} and observational estimates can be assigned to invariable moments of the modelled aerosol populations (the relative position between volume and surface distribution in the model does not vary much in the stratosphere). In reality, the different moments seem to be much more variable (bottom panel of Fig. 9 in HOM11), and QBO nudging apparently helps to improve the model results.

3.3 Number density

In previous sections, QBO effects on integrated aerosol quantities were examined. In the following we further investigate how the QBO affects the size of aerosols in the tropical LS by an analysis of anomalies induced in specific ranges of their size distribution. Therefore, the modelled size distribution is partitioned into four size ranges, equivalent to the four modes, which are commonly used to define an aerosol distribution (e.g. Seinfeld and Pandis, 2006). In this respect, nucleation mode aerosols refer to particles with radii smaller than 0.005 µm. The Aitken mode is defined as the range between 0.005 µm and below 0.05 µm and the accumulation mode between 0.05 µm and below 0.5 µm. The coarse mode considers aerosols with radii equal or larger than 0.5 µm.

Fig. 10 shows that QBO modulations ~~strongly differ~~ **are different** in the four modes. This was implicitly expressed also in Fig. 7 by the small differences in the anomalies in SAD for the two integration ranges (whole spectrum and aerosols larger than 50 nm). In contrast to SAD anomalies, relative QBO effects in aerosol number densities are much stronger.

As seen from the nucleation mode number density profile (Fig. 10a), **the model suggests that binary homogeneous nucleation (BHN) occurs in the tropical LS.** Below 50 hPa, several hundred nucleation mode aerosols are found per cm^{-3} in the simulation. Above 50 hPa, their number density rapidly decreases and is almost three orders of magnitude lower around 20 hPa and above. Since the BHN parametrisation depends on the ambient temperature and water vapour content, it is not surprising that the QBO may influence the particle formation process. **This is indicated by the strong QBO modulations (±50 %) we find in nucleation mode number densities between 50–30 hPa (Fig. 10b). At the higher levels, the increasing stratospheric temperature and the decreasing moisture content suppress BHN.** However, small fluctuations are even seen above 30 hPa, that indicate either rapid vertical transport of freshly formed nuclei is imposing those signatures or even in the central and upper regions of the Junge layer nucleation is triggered by QBO imposed temperature fluctuations on relatively short time-scales. We will further examine those relationships in Sec. 3.4. **Anomalies at 70 hPa are of similar strength but shifted in phase to anomalies above. Below that level, only irregular patterns have been inferred which do not correlate with the dissipating QBO signal nor with the inferred nucleation rate anomalies (compare Fig. 11b). The origin of these artefacts and their relation to seasonal variations in the TTL have not yet been understood and should be investigated in more detail in future studies. Statistical significance of the signatures is confined to levels between 70–40 hPa.** As a caveat it should be mentioned that the nucleation process of aerosols, in particular in the LS, is poorly understood. Therefore, the above relationships strongly rely on the assumptions we made in modelling the process and for the composition and size of nucleation mode aerosols.

Strong positive modulations, i.e. increased number densities, are seen in the larger three modes of the size distribution (Fig. 10d, f, h) during easterly QBO phases and above regions where the largest bulk mixing ratios are found (30 - 20 hPa). Anomalies in the coarse mode number density (Fig.

10h) appear somewhat irregularly in the lowest levels above the TTL. Here~~QBO effects infer~~, the QBO signal **interferes** with effects imposed by the annual cycle in the tropical tropopause, which has no definite synchronisation with the QBO phase (Baldwin et al., 2001). Above 70 hPa, coarse mode number density anomalies are positive during the time when easterly zonal wind prevails and may reach ±100 % in the evaporation region due to the low abundance of aerosol coarse mode particles there~~(Fig. 10g).~~ **, as seen from the climatological mean profile (Fig. 10g). Statistical significance is indicated only between 30–14 hPa, that is where such relatively heavy particles are quickly being removed by sedimentation.**

Alterations in the accumulation mode number density (Fig. 10c) are mainly confined to regions where the droplets evaporate and get smaller. **The relative strength of the anomalies increases almost linearly from ±5 % at 20 hPa to about ±100 % around 3 hPa.** In contrast to the coarse mode, from the climatological mean profile (Fig. 10e) it is obvious that at ~~those~~ the higher altitudes accumulation mode particles are still relatively abundant, although at least one order of magnitude less than further below, where the bulk mixing ratio is largest (Fig. 6a). ~~In the latter region, i.e. between 50 and 20 , relative modulations are below ±5 all the way down to the TTL.~~ **In the latter region and all the way down to the TTL, relative modulations are low as ±5 %. Statistical significance is indicated in three regions of the equatorial LS, that is in the lowest analyzed levels between 100–90 hPa, in central regions of the layer between 40–18 hPa as well as between 10–4 hPa.**

In the tropical LS, the Aitken mode aerosol concentration is largest just above the TTL, and rapidly decreases with increasing height (Fig. 10c). Collisional scavenging (coagulation) is responsible for the concentration decrease in the lower region of the layer, up to 30 hPa, while evaporation is a sink for both aerosol mass and number density above 20 hPa. Relative QBO modulations in the Aitken mode number density are quite strong throughout the entire tropical Junge layer. ~~Modulations~~ **They are not statistically significant in a layer between 25–10 hPa, that is where the climatological mean profile has almost no gradient. QBO signatures** of ±20 % are found between 50 and 30 hPa and reach ±100 % in the evaporation region. That is in contrast to the ~~other~~ previously discussed modes, the mixing ratio and the SAD, where strong relative modulations are confined to the upper regions of the layer (above 30 hPa). In addition, also the characteristic patterns of positive/negative anomalies and their phase reversal in the vertical make this particular QBO effect exceptional in comparison to the other analysed QBO effects on tropical LS aerosols. This result clearly indicates that QBO effects on aerosol processes in the tropical LS interact highly nonlinearly with each other.

~~As seen from the nucleation mode number density profile (Fig. 10a), binary homogeneous nucleation (BHN) can occur in the tropical LS. Below 50 , several hundred nucleation mode aerosols are found per in the model. Above 50 , their number density rapidly decreases and is almost three orders of magnitude lower around 20 and above. Since the BHN parametrisation depends on the ambient temperature and water vapour content, it is not surprising that the QBO may influence the particle~~

formation process, and this is presumably reflected here in the quite strong modulations of nucleation mode number densities (Fig. 10b). The anomalies are confined mainly to the region between 70 and 30 . Above this layer, the higher stratospheric temperature and lower moisture content more and more inhibit BHN. However, small fluctuations are even seen above 30 , that indicate either rapid vertical transport of freshly formed nuclei is imposing those signatures or even in the central and upper regions of the Junge layer nucleation is triggered by QBO imposed temperature fluctuations on relatively short time-scales. We will further examine those relationships in Sec. 3.4. As a caveat it should be mentioned that in particular the nucleation process of aerosols is poorly understood. Therefore, the above relationships strongly rely on the assumptions we made in modelling the process and for the composition and size of nucleation mode aerosols in the LS.

3.4 Microphysical processes

To reveal the mechanisms responsible for the QBO effects discussed above, we further examine how microphysical processes are affected by the QBO. Principally, the strength of aerosol microphysical processes depends on the thermodynamic state of the stratosphere. Temperature and the vapour contents of water and sulphuric acid determine the rate of formation of new aerosol, their growth and loss through reversible mass transfer between the gas and the liquid phase. Here, we do not consider aerosol growth by coagulation nor particle sedimentation since these processes have not been diagnosed from the model in a manner that would allow an examination of QBO signatures.

To reveal the mechanisms responsible for the QBO effects discussed above, we further examine how the QBO affects microphysical processes of transferring sulphur mass between the gas and the aerosol, i.e. nucleation and condensation/evaporation. Principally, the strength of the processes depends on the thermodynamic state of the stratosphere. The saturation of H_2SO_4 and H_2O, which depends on temperature and vapour concentrations, determines the rate of formation of new aerosol as well as their growth and loss through reversible mass transfer between the gas and the liquid phase. Coagulation and sedimentation are other important microphysical processes which shape size distributions (e.g. Jacobson, 2005) and limit the vertical extent of the aerosol layer (e.g. Kasten, 1968; Hamill et al., 1977, 1997) . Since both processes have not been diagnosed from the model in a way that will allow a consistent determination of their QBO signatures, in the following we are focussing on the discussion of QBO signals in aerosol nucleation and H_2SO_4 condensation/evaporation. Nevertheless, at the end of the section we make an attempt to estimate potential QBO effects on coagulation and sedimentation, because both processes have been explicitly considered in the model system and their (non-isolated) effects presumably superimpose other analysed QBO signatures.

3.4.1 Nucleation

In the lower tropical stratosphere, the modelled BHN rate after Vehkamäki et al. (2002), exhibits a maximum at 50 hPa (Fig. 11a). ~~Above 50 , it rapidly declines and tends to zero at 30 as in the CTL run (HOM11).~~ **The climatological mean profile has a sharp negative gradient above 50 hPa, and is not different from the CTL run (HOM11).** The pattern of ~~QBO induced~~ QBO-induced anomalies in the aerosol nucleation rate (Fig. 11b) correlates well with the QBO signature in the nucleation mode number density (Fig. 10b). ~~The cold anomaly at QBO east shear~~ **The cold anomaly in QBO easterly shear zones** imposes a 5 - 10 % amplification of the BHN rate around the 50 hPa pressure level. ~~Although this is not a large number, the respective increase in the nucleation mode number density can amount to 50 .~~ **Although this is not a large number, the respective increase in the nucleation mode number density can be as large as +50 % during times when QBO easterlies are strongest. During that time the layer approaches its lowest vertical expansion, so that the disproportional modulation in the number density of nuclei may arise from dampening the advective aerosol lofting or from QBO-induced downward transport (relative to the climatological mean state).** At 30 hPa and above no significant impact of the QBO on the BHN is found, so that respective signatures seen in the nucleation mode number density (Fig. 10b) ~~, as discussed in Sec. 3.3,~~ may have a different origin than new particle formation. QBO effects in the lowest regions of the LS ~~strongly~~ interfere with seasonal variations in the TTL, ~~so that the composite of~~ with the result that the composited QBO signatures in the BHN rate ~~appears~~ appear rather irregularly.

As discussed in Sec. 2.3, modelled QBO signatures in the tropical LS temperature show a warm bias compared to ERA-Interim in regions where BNH occurs. Assuming other properties remain constant, colder anomalies would foster BHN (Vehkamäki et al., 2002) . Therefore, it is likely that the modelled QBO signature in BHN may be underestimated, apart from uncertainties which remain for the rarely investigated process under stratospheric conditions. Statistical significance is indicated between 70–30 hPa, very similar to signatures in the nucleation mode number density.

3.4.2 Condensation of H_2SO_4

~~Following the approach of HOM11, we analyse QBO signatures in condensation and evaporation of aerosols in terms of a time-averaged molecule concentration that is transferred between the gas and the liquid phase.~~

Below 50 hPa, the model indicates that ~~condensation is quite strong, but it decreases rapidly with height as seen from the climatological mean profile of molecules that condenses onto aerosols (Fig. 11c).~~ **the H_2SO_4 condensable source rate (in units of $cm^{-3}\,s^{-1}$) is quite strong, but it decreases rapidly with height as seen from its climatological mean profile (Fig. 11c).** The

respective QBO signature (Fig. 11d) shows three regimes that are out of phase in the upper and lower regions of the Junge layer. Phase reversals occur around 15 hPa and between 7 and 5 hPa. **Only regions below 25 hPa are statistically significant.**

When easterly winds prevail at 50 hPa or below, positive anomalies in the ~~condensational growth~~ **condensable source rate** in the order of 5 - 10 % are induced by the QBO. Here, ~~QBO induced~~ QBO-induced cold anomalies in the stratospheric temperature (Fig. 2b) reduce the saturation vapour pressure of H_2SO_4 at the droplet surface that fosters condensation. Since in these regions the total aerosol number concentration is much larger than above, the aerosol provides a large surface area for condensing molecules (Fig. 7a), and is therefore a strong sink for the H_2SO_4 vapour.

However, relative QBO anomalies are much larger (about $\pm$ 60 %) in regions of the Junge layer where aerosols predominately release their mass into the gas phase, i.e. above 20 hPa (Fig. 11e). This indicates that both processes occur simultaneously in the time mean, and there is no sharp transition identifiable between regions where aerosols predominantly grow or shrink. Here, above 20 hPa, the reversible mass transfer of H_2SO_4 molecules is in a cyclic balance that depends on the strong in-phase relationship between the QBO modulated stratospheric temperature and the H_2SO_4 vapour pressure. QBO modulated upwelling through the tropical tropopause (Gray and Chipperfield, 1990; Seol and Yamazaki, 1998) may additionally contribute to QBO signatures in H_2SO_4 condensation and are further discussed in Sec. 3.7.

In the regions of the Junge layer where the mixing ratio and the number densities of intermediate size aerosol are sufficiently large, i.e. below 10 hPa, the QBO signatures ~~of condensation~~ **in the condensable source rate of $\mathbf{H_2SO_4}$** correspond well with those in the Aitken mode number density (Fig. 10d). At certain levels they also correspond with the signatures in the number densities of the accumulation mode (between 50 and 30 hPa) and the coarse mode (between the TTL and 70 hPa).

3.4.3 Evaporation of H_2SO_4

Above 20 hPa, the H_2SO_4 saturation vapour pressure at the surface of the droplets gets larger than the H_2SO_4 partial pressure due to the photochemical production of H_2SO_4, ~~so that~~ and aerosols evaporate quicker than at lower altitudes. The process reaches its maximum strength around 7 to 5 hPa (Fig. 11e). ~~Above that level, most of the sulphate mass remains in the vapour phase and evaporation from aerosols strongly decreases.~~ **Above that level, most of the sulphate mass remains in the vapour phase, so that the evaporation sink rate (in $\mathbf{cm^{-3}\,s^{-1}}$) of $\mathbf{H_2SO_4}$ molecules from the aerosols into the gas phase gets weaker with height.**

Due to the strong in-phase relationship between the H_2SO_4 vapour pressure and the QBO temperature signature, evaporation anomalies are also in phase with temperature anomalies imposed by the QBO. The model indicates that during the warm anomaly QBO westerly shear the process is fostered, while cold anomalies in the QBO easterly shear have a dampening effect. ~~Fig. 11d and Fig. 11f imply that the two intrinsically competing processes condensation and evaporation apparently occur~~

simultaneously. This mainly arises from the time-averaging (composited monthly means) of the two unidirectional flows, directed either into the gas phase or onto the aerosols. **The modulation is in the order of ±60 % at the highest temperature signatures. Statistical significance is indicated between 14–3 hPa.**

As mentioned before, the tropical Junge layer has a much larger variability in the QBO-nudged simulation than in the CTL simulation. In the QBO experiment, the balance in the mass transfer is shifted towards evaporation above 10 . Although evaporation impose a decrease in the SAD (the total number of aerosols remains constant when they evaporate or even decreases due to complete evaporation) that is compensated in the QBO experiment by the QBO modulation of the advection of small aerosols. This results in a positively modulated SAD in the QBO easterly shear above 10 (Fig. 7). **Fig. 11d and f imply that the two intrinsically competing processes condensation and evaporation appear simultaneously. This effect arises mainly from the time averaging of the data, to lesser extent also from zonal averaging. Nevertheless, condensation and evaporation compete on the process level in the model and are characterised by their unidirectional molecular flows either onto or away from the particles. Although equally phased anomalies may overlap partially in the residual composites, an analysis of their QBO signatures is still possible since both processes have been diagnosed from individual output channels during model integration time. We infer, indeed, a remarkable feature in the coupling of the two processes in comparison to the CTL simulation without a QBO: in the QBO-nudged simulation the balance of the H_2SO_4 mass transfer is shifted towards evaporation above 10 hPa. This is because the tropical Junge layer has a much larger variability in the QBO-nudged simulation than in the CTL simulation. In principle the process of evaporation decreases the SAD (the total number of aerosols remains either constant when they evaporate or decreases due to complete evaporation), but in the QBO experiment this effect is partly compensated by the QBO modulated vertical advection of small aerosols. This results in a positively modulated SAD in the QBO easterly shear above 10 hPa (Fig. 7).**

It should be mentioned ,that compared to the ERA-Interim reanalysis, modelled QBO temperature anomalies are up to 2 K smaller below the 10 hPa pressure level (Fig. 2a, b) and 1 – 2 1–2 K larger above 10 hPa, where evaporation occurs. Thus, in the model the net effect of QBO on the evaporation of sulphate droplets may be overestimated to some degree. **Thus, in the model the net effect of QBO on the counteracting processes evaporation and condensation of H_2SO_4 may be overestimated to some degree. On the other hand, due to the large QBO induced variations of the Junge layer's upper lid, presumably temperature-related biases in the modelled QBO interactions are more pronounced for evaporation. That is because the process ultimately determines the maximum altitude of the layer's upper lid, dependent on the saturation state and the thermodynamic stability of aerosol.**

3.4.4 Coagulation and Sedimentation

Although not diagnosed in the same manner as the H_2SO_4 mass transfer, some aspects about the interference between the QBO and the coagulation and sedimentation processes can be derived from first principles, causal relationships of the atmospheric aerosol system (e.g. Seinfeld and Pandis, 2006; Hamill et al., 1997) and our results. Both processes have been modelled together with the other three processes (nucleation, condensation, evaporation), as described above. It is important to bear in mind that coagulation is a mass conserving process, affecting the number of aerosols (predominately the smallest, a review is found e.g. in Jacobson (2005)). In contrast, sedimentation is a sink for both mass and number of aerosols (e.g. Hamill et al., 1977) .

Since sedimentation is predominantly limiting the Junge layer's vertical extent (the strength of the sink increases almost linearly with altitude), mainly the aerosol layer's upper lid is supposed to be affected by QBO modulations of sedimentation. According to first principles, an Aitken mode aerosol of 10 nm radius settles about 0.1 $\mathrm{km\,month^{-1}}$ at 10 hPa and an accumulation mode aerosol with 100 nm radius settles about 8 times faster ($\sim 0.8\,\mathrm{km\,month^{-1}}$). The rate approximately doubles when the aerosol is lofted by 3 km over 3–4 months, as indicated by our model during the QBO east phase (Fig. 5b). Note, that this result already incorporates the effect of the QBO on sedimentation. Since larger aerosols are relatively abundant at 10 hPa and above (Fig. 10e and top left panel of Fig. 13), the numbers imply an effective sedimentation sink for larger aerosols, counteracting the aerosol lofting by the QBO. This relationship can be understood as in indirect signature of the QBO on the sedimentation flux of particles from the upper region of the Junge layer. A second order, direct effect on the sedimentation of LS aerosols is also conceivable, that is the imposed QBO signature on the dynamic viscosity of air, determining the falling speed of an aerosol. This modulation may occur via the 1–2 K modulation of the tropical stratospheric temperature in regions where the sedimentation sink is large enough to play a role. In our model we used the parametrisation of Pruppacher and Klett (1979) , suggesting that a QBO signature in the dynamic viscosity of air is $\ll 1\,\%$. Hence, the signal is considerably small and presumably not distinguishable from other signals.

QBO effects on the process of aerosol coagulation may also be divided into direct and indirect effects. A potential direct QBO signature occurs via modulation of the (Brownian) diffusion coefficient of the aerosol due to the imposed temperature anomalies and the coefficient's dependence on altitude. The effect is potentially not negligible above 10 hPa where air is less dense and the Knudsen number (ratio between the mean free path of air molecules to the aerosol size) is approximately one order of magnitude larger than at 100 hPa. A more distinct signature, however, seems to be plausible through indirect QBO modulations via the pathway of triggering new particle formation, as discussed above, and their subsequent coagulation.

Potentially also vertical advection of nuclei contributes to this indirect QBO effect, because also the sedimentation sink of the smallest aerosol increases rapidly if they are lofted.

Further studies are needed to understand the complex and partly nonlinear relationships of these respective QBO effects that may be of particular importance when geoengineering options are investigated.

3.5 Particle properties

Aerosols in the stratosphere become more concentrated with height until the increase in the H_2SO_4 saturation vapour pressure at the surface of the droplet sets an upper limit to the thermodynamic stability of the droplets. The concentration change of the droplet solution is obvious from the climatological mean tropical profiles of the binary solution density (Fig. 12a), the sulphuric acid weight percentage of the droplets (Fig. 12c), and their water content (Fig. 12e). The latter is expressed as the relative difference to a representative Junge layer aerosol mean state as it is widely used in literature (density of 1.7 $\mathrm{g\,cm^{-3}}$, sulphuric acid weight percentage of 0.75; see e.g. Rosen, 1971; Hamill et al., 1997).

Changes in the aerosol composition play an important role for understanding seasonal variations of observed aerosol optical properties (e.g. Yue et al., 1994; Hamill et al., 1997). Since equilibrium with respect to water is achieved quasi-instantaneously also in the relatively dry stratosphere, small variations in the water content forced by the QBO may additionally contribute to QBO signatures in the droplet composition that arise from ~~QBO induced~~ QBO-induced temperature anomalies or advection due to the residual circulation of the QBO.

Residual QBO anomalies of the diagnosed particle properties (Fig. 12b, d, f) indeed reveal a strong analogy to ~~QBO induced~~ QBO-induced temperature anomalies of the tropical stratosphere (Fig. 2b). Aerosols have a higher sulphuric acid weight percentage during times when positive temperature anomalies are induced during the QBO westerly shear. Although respective relative modulations almost linearly scale with the QBO temperature signal, in the order of approximately $\pm 1\%$, this has extensive consequences for aerosol microphysics above the 20 hPa pressure level~~because~~. Because it facilitates evaporation and reduces the SAD. The opposite occurs in the relatively cold QBO east shear. **All QBO signatures are statistically significant up the 7 hPa pressure level.**

~~In the lower regions, where evaporation is negligible and the mixing ratio is much larger, i.e. below 20 , this QBO effect interferes with effects imposed by the annual cycle in the modelled stratospheric temperature. During the summer months, when the temperature in the upwelling branch of the BDC increases by 2 - 6 , relative to winter conditions, sulphate droplets maintain their equilibrium with the ambient air through the release of and molecules so that they get smaller (Steele and Hamill, 1981) .~~ **The analysed aerosol properties are also modulated by changes due to seasonal variations in the stratospheric temperature (e.g. Steele and Hamill, 1981; Yue et al., 1994) . Since the latter are stronger above the TTL than in the middle stratosphere, seasonal variations in the aerosol**

properties play a particular role below the evaporation region. For instance, at 70 hPa the sulphuric acid weight percentage and water content vary between summer and winter by about 20 % (not shown), and the density of the droplet solution by ~ 6 %. At 10 hPa the variations do not exceed 1–2 %. Hence, below approximately 20 hPa, these variations are up to a magnitude stronger than the inferred QBO signatures. This is clearly different from the aerosol mixing ratio (Fig. 4), where only below 70 hPa seasonal variations are (approximately two times) stronger than the QBO signal.

3.6 Size distribution

The QBO imprint in modelled aerosol size distributions is shown in Fig. 13 for QBO east phases, exemplarily for pressure levels of 10 and 40 hPa. Signatures in QBO west phases have an opposite sign (not shown). The upper panels depict size distributions from linear interpolations between adjacent bins in terms of number concentrations ($\mathrm{particles\,cm^{-3}}$). To better illustrate the QBO effect, the bottom panels show relative differences per bin as bar charts. The bars are colour coded by aerosol modes, as discussed in Sec. 3.3. As before, all data are monthly zonal means between 5°N–5°S. In order to provide an independent diagnostics, we sampled the data according to the sign of the QBO east phase zonal wind tendency dU_{EQBO}/dt, and not according to the sign of the QBO signatures we inferred for integrated quantities above. In the averages only easterlies $> |4|$ $\mathrm{m\,s^{-1}}$ are considered.

The size distribution curves (top panels) do not differ much due to the double logarithmic scale. The relative differences between the curves (bottom panels), however, show sufficiently large QBO signatures, which are consistent with our findings from integrated parameters. In particular they correspond well with mode-wise integrated number densities (Fig. 10): At 10 hPa, more aerosols (except in the coarse mode) are found when the zonal wind tendency is positive (black curve). This corresponds to positive anomalies in the Aitken and accumulation mode (Fig. 10d and f) in the month after the transition from the QBO westerly to the easterly phase. Nucleation and coarse mode signatures are not significant at this level (Fig. 10a, g). At 40 hPa, larger concentrations are found during months when the easterly zonal wind is getting weaker (negative tendency, gray curve). This corresponds to positive anomalies in the Aitken and accumulation mode number densities in the month before the onset of the westerly zonal wind transition (Fig. 10d and f). Only aerosols of intermediate size, i.e. the largest Aitken mode and smallest accumulation mode particles, are inversely modulated. Here, the 7–month phase lag of accumulation mode QBO signatures, with respect to the Aitken mode, are canceling out respective signatures in the size distribution averages. In contrast to 10 hPa the signature in the nucleation mode is statistically significant, in addition BHN may be triggered by the QBO in their easterly phase (Fig 10b).

The exemplarily shown size distributions and their relative changes also contain the imprint

of QBO modulations in the microphysical processes, as discussed above, and correspond to signatures in the surface area density (Sec. 3.2.1): At the lower level, condensation is strong and shows a positive anomaly when $dU_{EQBO}/dt < 0$ (month with accelerating easterlies; compare anomalies in Fig. 11d). Accordingly, the SAD is positively modulated. Particularly, the effect is larger when the SAD is inferred for the entire range of aerosols (Fig. 7b) and weaker in the adopted size range with R $\geq$ 50 nm (Fig. 7d). At 10 hPa, condensation is approximately still one order of magnitude stronger than evaporation in the time-mean (Fig. 11c, e). This is also reflected in the size distributions, where the positively modulated condensational growth during months when $dU_{EQBO}/dt < 0$ causes a shift of fine mode aerosols to the right (gray curve). However, this growth is likely be competing with coagulation. That is because coagulation causes the net-loss in the number concentration for aerosols with R $<$ 50 nm (note, H_2SO_4 condensation is aerosol number conserving), see also discussion in Sec. 3.4.4.

Not equally distributed QBO signatures in the size distributions also refer to the above mentioned nonlinear coupling between the processes which determine the size distribution's shape, and, in turn, QBO signatures in the different aerosol modes and various properties. Hence, supporting our view that only by consideration of the QBO the variability of the lower stratospheric aerosol layer in the tropical LS is modelled adequately. Otherwise a comparably static Junge layer with a distinctly different life cycle of aerosols is simulated, with possibly false implications.

3.7 Precursor Gases

Previous work already addressed some aspects of the natural variability of aerosol precursors in the stratosphere. HOM11, for example, discussed in detail how the QBO-free model predicts the aerosol precursors SO_2 and sulphuric acid vapour in the stratospheric background in comparison to observations. Brühl et al. (2012) analysed the modelled short term variability of SO_2 and sulphuric acid vapour with respect to oxidising capabilities of OCS in the volcanically quiescent stratosphere from 1999 and 2002. But Brühl et al. (2012) did not in greater detail investigate the coupling between the aerosol layer, the precursors and the QBO.

Generally, little is known about the vertical profiles of SO_2 and H_2SO_4 vapour in the stratosphere. Most measurements were conducted in the early years of systematic exploration of the stratosphere (SPARC/ASAP, 2006; Mills et al., 2005, HOM11). During the last two decades the majority of observations of sulphur bearing gases were conducted in the troposphere. According to SPARC/ASAP (2006) less than a quarter of the campaigns measured in the lowermost stratosphere. In the more recent years, SO_2 measurements were conducted on a more ~~regularly~~ regular base, e.g. when aircraft campaigns touched the lowermost stratosphere (e.g. during SOLVE). But those are predominately confined to the lowermost regions of the mid- and high latitudes, so that they cannot be taken into

consideration within this study that focus on the tropical LS. Above 30 km data from only one campaign was available until last year (2013) that measured SO_2 in the NH subtropics (ATMOS infrared spectrometer on a NASA Space Shuttle in 1985; Rinsland et al., 1995). Recently a climatology of monthly and zonal mean profiles of SO_2 volume mixing ratios has been derived from Envisat/MIPAS measurements in the altitude range 15 - 45 km for the period from July 2002 to April 2012 (Höpfner et al., 2013). **We compare to this dataset below.** Only a few extra-tropical data are available for H_2SO_4 vapour and are discussed in Mills et al. (2005) and HOM11.

In the model, the climatological mean SO_2 mixing ratio (Fig. 14a) rapidly decreases from the TTL to $\sim$ 50 hPa due to rapid photochemical conversion to H_2SO_4~~(Fig. ??a).~~ . Above 50 hPa, the mixing ratio increases due to the oxidation of OCS. Above 10 hPa the photolysis of H_2SO_4 vapour establishes an upper-stratospheric reservoir of SO_2, which plays a large role in the triggering of new aerosol formation in the polar spring stratosphere when the sunlight returns ~~(Mills et al., 1999, 2005, HOM11) .~~ (Mills et al., 1999, 2005; Campbell et al., 2014, HOM11) . **The MIPAS profile varies much less than the modelled one. Quantitatively, MIPAS mixing rations are an order of magnitude larger around 40 hPa and factor 2 larger between 25 and 7 hPa. The origin of this discrepancy remains unclear. But since both Höpfner et al. (2013) and HOM11 (CTL simulation) emphasised a good agreement to the subtropical SPACELAB3/ATMOS SO2 profile (26–32N), potentially our model overestimates the annual cycle in the tropical SO2 profile, the photochemical SO2 oxidation, or both. On the other hand, we cannot prove tropical MIPAS profiles in more detail since other continuous measurements well above the TTL do not exist. Further investigations and other data sources are needed to understand this behaviour.**

The modelled climatological mean tropical H_2SO_4 vapour mixing ratio profile (Fig. ~~??c~~15a) exhibits a minimum slightly above the 50 hPa pressure level, where the vapour rapidly condenses onto aerosols. Above 50 hPa, the saturation vapour pressure of H_2SO_4 rapidly increases (between 50 and 10 hPa by 7 orders of magnitude) so that with increasing altitude less vapour condenses and most of it remains in the gas phase. Above 20 hPa, the probability of droplet evaporation gradually increases with height, so that the gradient in the sulphuric acid vapour mixing ratio further increases to around the 5 hPa level. That is the altitude where H_2SO_4 photolysis to SO_3 becomes important (Burkholder and McKeen, 1997). SO_3 in turn is photolysed to SO_2 and builds up the SO_2 reservoir in the upper stratosphere. This is seen in most of the stratosphere-resolving (chemistry-) climate models with an interactive aerosol component (Turco et al., 1979; Weisenstein et al., 1997; Mills et al., 2005, HOM11). Envisat/MIPAS observations recently confirmed the existence of such a reservoir (Höpfner et al., 2013), that has been already indicated by ATMOS measurements in spring 1985 at northern hemispheric subtropical latitudes. Above 45km, however, the ATMOS profile implies a further sink for SO_2 near the stratopause by largely decreasing mixing ratios above 48 km ($\sim$ 1 hPa), that is not confirmed by most models.

As seen from Fig. ~~??b and Fig. ??d~~14b and c, as well as from Fig. 15b, the QBO similarly

modulates to a large degree SO_2 and H_2SO_4 vapour in the equatorial stratosphere. Just above the TTL we found deviations from the modelled climatological mean of up to $\pm 20\%$. Above 20 hPa, the relative QBO signature may reach $\pm 50\%$. While below 50 hPa, positive (negative) anomalies correlate with easterly (westerly) winds, the anomalies above relate to the QBO shear, hence, are in-phase with the QBO temperature signal. A phase shift in the anomalies is found at approximately 10 hPa in SO_2 and in H_2SO_4 vapour around the 3 hPa pressure level. ~~Höpfner et al. (2013) report QBO signatures in MIPAS observed of 15- 20 between 30 and 37 altitude at the equator between 10°S-10°N, that is 30 - 50 of the observed climatological means.~~

QBO anomalies in the tropical MIPAS SO_2 climatology are relatively irregular below the 50 hPa pressure level. Here, volcanic perturbations may have an imprint in the derived QBO signature. It is not trivial to remove such irregularly appearing pattern from the climatology. Because such signatures disperse spatially, propagate up in-time, and generally decay in strength due to the relatively small chemical time constant (∼1 month; SPARC/ASAP, 2006) . More research is needed to establish a robust quantification method for the different factors determining the characteristics of the observed SO_2 time-series. Although above 50 hPa (∼20 km) the volcanic imprint is still detectable in the climatology (Höpfner et al., 2013, bottom panels in their Fig. 4 and 5) , we infer well defined QBO anomalies which correlate well with the QBO wind regime. This is different in the simulation, where SO_2 anomalies above 20 hPa lag behind the occurrence of strongest zonal winds. The relative strength of the anomalies is approximately similar in both datasets. Höpfner et al. (2013) reported QBO signatures in their MIPAS climatology as large as 30–50 %, relative to the climatological mean, being in good agreement with our analysis. MIPAS QBO anomalies are significant only between 50–18 hPa, whereas modelled anomalies are significant between 90–30 hPa and above 3 hPa. At this point, we do not understand in particular the lag of the MIPAS anomalies relative to the model. Differences in the phase-shifts of the inferred anomalies in the vertical are explained by the different shapes of the profiles. As mentioned above, the modelled photochemistry and/or model deficits in the representation of the annual cycle of the tropical upwelling may explain, at least parts, of the described differences in the inferred QBO signatures.

Below the QBO easterly jet upwelling is enhanced (Gray and Chipperfield, 1990; Seol and Yamazaki, 1998), hence positive precursor anomalies below 50 hPa ~~pressure level reflect~~ depict an enhanced vertical transport through the TTL in the model. To what extent H_2SO_4 vapour is transported from the free troposphere into the LS remains speculative, because the small chemical time constant of H_2SO_4 vapour in the LS (∼1 day) implies that H_2SO_4 vapour anomalies may appear as finger-print structures of the SO_2 anomalies. This is also supported by the kinetics of the H_2SO_4 vapour forming reaction between SO_3 (oxidised from SO_2) and H_2O, that depend exponentially on $1/T$ (Sander et al., 2006), hence benefit from cold anomalies induced in the cold lowermost tropical stratosphere during QBO east phases.

Above 50 hPa, where modelled anomalies in both gases correlate well with the equatorial QBO temperature signal, it seems plausible that some of the H_2SO_4 vapour anomalies arise implicitly from the QBO modulated SO_2 oxidation. Phase reversal of the anomalies occur where the mixing ratio profile distinctly changes shape, thus indicate that QBO modulated advective transport accounts for most of the calculated QBO anomalies in the two precursor gases.

Furthermore, modelled QBO anomalies in the two precursor gases are in-phase with modulations in the Aitken mode aerosol number density (Fig. 10d) and the H_2SO_4 vapour ~~that condenses~~ condensing onto aerosols (Fig. 11d). This implies that pre-existent or newly formed aerosols rapidly grow by H_2SO_4 condensation, even though the strength of condensation decreases rapidly with height (Fig. 11c). ~~Together with in-phase anomalies in the nucleation rate and nucleation mode number density around 50 , this indicates that to a certain extent the origin of Aitken mode aerosols in the LS is not the free troposphere, from where they have been more rapidly uplifted when the QBO phase is easterly.~~ **Together with in-phase anomalies in the nucleation rate and nucleation mode number density around 50 hPa, this result indicates that, at least partly, the origin of Aitken mode aerosols in the LS is not the free troposphere, from where they have been more rapidly uplifted when the QBO phase is easterly. However, we cannot provide an more detailed quantification of pathways maintaining the volcanically quiescent aerosol layer in the tropical stratosphere, because it would require that OCS, one of the major sulphur sources in the LS (e.g. SPARC/ASAP, 2006) , needs to be treated prognostically (e.g. Brühl et al., 2012) . As a caveat it should be mentioned that the use of climatological mean oxidant fields potentially damp the simulated QBO effects in the precursors, since the fields do not contain inherent QBO signatures due to the averaging. We expect that a QBO-resolving and interactively coupled chemistry–aerosol model may show stronger precursor modulations because it would better capture the oxidising pathway from precursors to sulphate aerosols via O_x, OH, and NO_2.**

4 Conclusions

Here, for the first time, we provide model-based indications for concurrent QBO imposed effects in the tropical stratospheric aerosol layer that ~~shape~~ modulate the aerosol size distribution in a ~~highly~~ nonlinearly manner. Such effects have only been suggested so far from satellite-measured aerosol extinction coefficients (Trepte and Hitchman, 1992) ~~.~~ **and SO_2 measurements (Höpfner et al., 2013) .** Eleven years (1996–2006) of the post-Pinatubo stratospheric background were simulated with the aerosol-coupled middle-atmosphere circulation model MAECHAM5-SAM2. The data were examined with regard to the long-term variability of aerosol and precursors in the tropical lower stratosphere and variations caused by the QBO in aerosol dynamics and composition. We compared the data to a control simulation that did not resolve the QBO (HOM11), ~~and to merged data sets~~ to

merged datasets from observations of the solar occultation SAGE II satellite sensor and the space-borne CALIOP lidar ~~.~~ **and to the MIPAS observations of SO_2 from Höpfner et al. (2013) .**

There is a general agreement that the QBO is an important forcing mechanism of the Earth's climate (e.g. Baldwin et al., 2001; Brönnimann, 2007) and largely determines the global dispersion of stratospheric trace constituents (see Baldwin et al., 2001). However, accompanying effects on sulphate aerosol droplets that form the Junge layer in the stratosphere have not yet been addressed in detail. ~~In this paper, we~~ **Since this paper is a first attempt to examine the QBO-aerosol microphysics relationship in the tropical LS, we utilise a model system of reduced complexity with respect to the stratospheric aerosol system. We concentrate here on the simulation of sulphate aerosols since they dominate the stratospheric aerosol load. Other particulate substances might however have an impact on stratospheric dynamics as well. A more detailed understanding of the dynamics of sulphate aerosols in the tropical LS is also of particular interest for research on the separation of volcanic signatures from the natural variability of the stratospheric background, and is, therefore, a necessary step towards a better understanding of the aerosol behaviour in the LS as observed in the recent past.** We have shown that in the model the tropical Junge layer is ~~heavily~~ influenced by the QBO. The vertical expansion of the modelled layer, i.e. its thickness, differs by at least 5 km dependent on the phase of the QBO. This is in agreement with satellite observed aerosol extinctions and derived aerosol sizes, hence, does not arise solely from volcanic disturbances of the tropical lower stratosphere as argued by Hasebe (1994). This is important for understanding the climatological relevance of stratospheric background aerosols, which is still debated (e.g. Hofmann, 1990; Deshler et al., 2006; Solomon et al., 2011; Neely et al., 2013).

We found that the QBO affects all parameters we diagnosed from the model's aerosol scheme. Our results indicate that QBO effects in the sulphate droplet composition are ~~rather~~ small and depend almost linearly on the QBO signature in the tropical stratospheric temperature. QBO modulations in the modelled aerosol mixing ratio and size appear to be stronger and increase in the upper levels of the Junge layer (above 20 hPa), where the droplets evaporate. In particular at these altitudes we found clear indications for non-linear relationships in the aerosol processing due to the influence of the QBO. Furthermore, and in agreement with other studies, we found an enhanced upwelling of SO_2 into the lower stratosphere below the 50 hPa pressure level when the QBO is in its ~~east phase.~~ **easterly phase.** Our model indicates that this modulation in the supply of the SO_2 precursor establishes a chain of subsequent in-phase modulations in other modelled quantities below 50 hPa. The sulphuric acid vapour concentration is enhanced during easterly QBO and also the subsequent condensation onto intermediate sized aerosols in the Aitken mode. **QBO signatures in SO_2 are quantitatively in agreement with MIPAS observations from Höpfner et al. (2013) above the 50 hPa pressure level. However, it is not yet clear from our comparison, why the tropical climatological mean profiles differ substantially in their vertical shape. This difference may be responsible for the phase-lag of the QBO signatures between the**

model and MIPAS. The reduction of the stratospheric chemistry system to the sulphur cycle and pre-calculated monthly mean oxidant fields may partly explain the differences, but it shall be noted that our model's SO_2 profile is in the bulk of solutions from global stratospheric aerosol models. Other systematically observed SO_2 profile climatologies do not exist for the stratosphere, so that more research is needed to better understand this issue.

Compared to the CTL experiment, where the Junge layer behaves almost statically, the nature of the more realistically predicted Junge layer in the QBO experiment is predicted to be highly variable. Prevailing westerly zonal winds expand the layer in the vertical. This motion subsequently is backed by an adiabatically uplift of aerosols in the anomalously cold QBO easterly shear. With progressing downward motion of descending easterly zonal winds, the entire layer descends and vertically diverges due to advection imposed by the QBO meridional circulation overlying the BDC. Before the QBO westerly jet propagates through the layer, reduced upwelling below the jet is further displacing the layer down to lower altitudes, where the layer has its smallest vertical extension.

Resulting anomalies in the modelled tropical aerosol mixing ratio are very similar to those observed in ozone~~, hence~~. Hence they are dominated by QBO effects on the advective transport and are confined by the structure of the tropical mixing ratio profile~~in the tropics and exhibit a positive gradient above the TTL and a negative gradient above the mixing ratio maximum~~. In the upper levels of the Junge layer, integrated aerosol size quantities are much stronger modulated by the QBO than the bulk mixing ratio because imposed effects on microphysical processes play a larger role than further below. ~~The model predicts that the QBO modulates also the balance of between the gas and the droplet's liquid phase. Mass~~ **This view is confirmed by QBO signatures in the CCMI SAD, a merged dataset derived from satellite observations of aerosols extinction coefficients and backscatter from the SAGEII and CALIOP instruments. In particular in the evaporation region of the Junge layer the statistically significant signatures agree well. Below that level anomalies in the observation dataset are significantly stronger than in the model (~60 %), presumably due to volcanic signatures.**

The model predicts that the QBO modulates the balance of the mass transfer of H_2SO_4 vapour between the gas and the droplet's liquid phase. The mass transfer is shifted towards evaporation in the ~~QBO nudged~~ QBO-nudged model, compared to the CTL simulation. However, in the time average, evaporation is continuously accompanied by recurring condensation of H_2SO_4 onto the aerosols. The model indicates that below the evaporation region nucleation of particles is triggered by the QBO and may significantly influence the aerosol size distribution. However, this result strongly relies on use of the Vehkamäki-parametrisation of binary homogeneous nucleation of the sulphuric acid-water mixture in the model. ~~QBO effects on the extra-tropical Junge layer were not at the scope of this study. Further investigations follow to examine respective relationships.~~

Our simulation shows that the life cycle of sulphate droplets in the tropical LS is determined by processes which are coupled in a strongly non-linearly manner to the QBO. This is because

imposed QBO signatures in the different aerosol properties differ (i) in strength, (ii) differ over the size range of aerosols, (iii) are a function of altitude, and (iv) may be shifted in phase. It is clear, that away from the equatorial belt QBO signatures in LS aerosol may show other signatures and couplings due to phase-shift of the extratropical QBO signal, which also weakens poleward (Baldwin et al., 2001) . QBO effects on the extra-tropical Junge layer were not at the scope of this study. Further studies follow to examine respective relationships.

The complexity of the described interactions between the QBO and the Junge layer in the model might be a key aspect in attempts to understand the global impact of stratospheric aerosols. It may also help to assess the discrepancy between modelled and observed aerosol quantities in periods when the stratosphere is largely unperturbed by sporadic injections from volcanoes or other sources. Although not addressable with this model configuration, the catalytic cycles that destroy wintertime polar stratospheric ozone may respond to QBO effects in the Junge layer. And, moreover, it seems likely that such effects may feed back into the climate system, further complicating the comprehensive understanding of the aerosol system in the UTLS.

Acknowledgements. We like to ~~greatly~~ acknowledge Christian von Savingy, Lena A. Brinkhoff, Beiping Luo, Abhay Devasthale, Hauke Schmidt, Steffan Kinne, Hartmut Graßl, Ulrike Niemeier, and Kathryn Emmerson on their helpful comments on the manuscript. We thank the two anonymous reviewers for their valuable comments and suggestions. We also gratefully acknowledge Michael Hoepfner (and the KIT) for providing the MIPAS data and his kindly help. Simulations were done at the German Climate Computer Center (DKRZ). Parts of the work have been funded by the German Federal Ministry of Education and Research (BMBF) under the ~~project ROSA (funding reference code~~ projects ROSA (FKZ: 01LG1212A) and MIKLIP (FKZ: 01LP1130A).

References

Andrews, D. G., Holton, J. R., and Leovy, C. B.: Middle Atmosphere Dynamics, Academic Press, San Diego, CA, 1987.

Arfeuille, F., Luo, B. P., Heckendorn, P., Weisenstein, D., Sheng, J. X., Rozanov, E., Schraner, M., Brönnimann, S., Thomason, L. W., and Peter, T.: Modeling the stratospheric warming following the Mt. Pinatubo eruption: uncertainties in aerosol extinctions, Atmospheric Chemistry and Physics, 13, 11 221–11 234, doi:10.5194/acp-13-11221-2013, http://www.atmos-chem-phys.net/13/11221/2013/, 2013.

Baldwin, M. P. and Gray, L. J.: Tropical stratospheric zonal winds in ECMWF ERA-40 reanalysis, rocketsonde data, and rawinsonde data, Geophys. Res. Lett., 32, L09 806, doi:10.1029/2004GL022328, 2005.

Baldwin, M. P., Gray, L. J., Dunkerton, T. J., Hamilton, K., Haynes, P. H., Randel, W. J., Holton, J. R., Alexander, M. J., Hirota, I., Horinouchi, T., Jones, D. B. A., Kinnersley, J. S., Marquardt, C., Sato, K., and Takahashi, M.: The quasi–biennial oscillation, Rev. Geophys., 39, 179–229, 2001.

Barnes, J. E. and Hofmann, D. J.: Variability in the stratospheric background aerosol over Mauna Loa observatory, Geophys. Res. Lett., 28, 2895–2898, 2001.

Bauman, J. J., Russell, P. B., Geller, M. A., and Hamill, P.: A stratospheric aerosol climatology from SAGE II and CLAES measurements: 1. Methodology, J. Geophys. Res., 108, 4382, doi:10.1029/2002JD002992, 2003a.

Bauman, J. J., Russell, P. B., Geller, M. A., and Hamill, P.: A stratospheric aerosol climatology from SAGE II and CLAES measurements: 2. Results and comparisons, 1984–1999, J. Geophys. Res., 108, 4383, doi:10.1029/2002JD002993, 2003b.

Bourassa, A. E., Robock, A., Randel, W. J., Deshler, T., Rieger, L. A., Lloyd, N. D., Llewellyn, E. J. T., and Degenstein, D. A.: Large Volcanic Aerosol Load in the Stratosphere Linked to Asian Monsoon Transport, Science, 337, 78–81, doi:10.1126/science.1219371, 2012.

Brönnimann, S.: The impact of El Niño-Southern Oscillation on European climate, Rev. Geophys., 45, RG3003, doi:10.1029/2006RG000199, 2007.

Brühl, C., Lelieveld, J., Crutzen, P. J., and Tost, H.: The role of carbonyl sulphide as a source of stratospheric sulphate aerosol and its impact on climate, Atmospheric Chemistry and Physics, 12, 1239–1253, doi:10.5194/acp-12-1239-2012, http://www.atmos-chem-phys.net/12/1239/2012/, 2012.

Burkholder, J. B. and McKeen, S.: UV absorption cross sections for SO_3, Geophys. Res. Lett., 24, 3201–3204, 1997.

Butchart, N., Scaife, A. A., Austin, J., Hare, S. H. E., and Knigh, J. R.: Quasi–biennial oscillation in ozone in a coupled chemistry–climate model, J. Geophys. Res., 108, 4486, doi:10.1029/2002JD003004, 2003.

Campbell, P., Mills, M. J., and Deshler, T.: The global extent of the mid stratospheric CN layer: A three-dimensional modeling study, J. Geophys. Res., 119, 1015–1030, doi:10.1002/2013JD020503, 2014.

Choi, W., Grant, W. B., Park, J. H., Lee, K., Lee, H., and Russell III, J. M.: Role of the quasi-biennial oscillation in the transport of aerosols from the tropical stratospheric reservoir to midlatitudes, J. Geophys. Res., 103, 6033–6042, 1998.

Choi, W., Lee, H., Grant, W. B., Park, J. H., Holton, J. R., Lee, K.-M., and Naujokat, B.: On the secondary meridional circulation associated with the quasi-biennial oscillation, Tellus B 54, 4, 395–406, 2002.

Damadeo, R. P., Zawodny, J. M., Thomason, L. W., and Iyer, N.: SAGE version 7.0 algorithm: ap-

plication to SAGE II, Atmospheric Measurement Techniques Discussions, 6, 5101–5171, doi:10.5194/amtd-6-5101-2013, 2013.

Dentener, F., Kinne, S., Bond, T., Boucher, O., Cofala, J., Generoso, S., Ginoux, P., Gong, S., Hoelzemann, J., Ito, A., Marelli, L., Penner, J., Putaud, J.-P., Textor, C., Schulz, M., Werf, G., and Wilson, J.: Emissions of primary aerosol and precursor gases in the years 2000 and 1750 - prescribed data–sets for AeroCom, Atmos. Chem. Phys., 6, 4321–4344, 2006.

Deshler, T., Hervig, M. E., Hofmann, D. J., Rosen, J. M., and Liley, J. B.: Thirty years of in situ stratospheric aerosol size distribution measurements from Laramie, Wyoming (41° N), using balloon–borne instruments, J. Geophys. Res., 108, doi:10.1029/2002JD002514, 2003.

Deshler, T., Anderson-Sprecher, R., Jäger, H., Barnes, J., Hofmann, D. J., Clemesha, B., Simonich, D., Osborn, M., Grainger, R. G., and Godin-Beekmann, S.: Trends in the nonvolcanic component of stratospheric aerosol over the period 1971–2004, J. Geophys. Res., 111, D01 201, doi:10.1029/2005JD006089, 2006.

Dubovik, O., Smirnov, A., Holben, B. N., King, M. D., Kaufman, Y. J., Eck, T. F., and Slutsker, I.: Accuracy assessments of aerosol optical properties retrieved from Aerosol Robotic Network (AERONET) Sun and sky radiance measurements, J. Geophys. Res., 105, 9791–9806, 2000.

English, J. M., Toon, O. B., Mills, M. J., and Yu, F.: Microphysical simulations of new particle formation in the upper troposphere and lower stratosphere, Atmospheric Chemistry and Physics, 11, 9303–9322, doi:10.5194/acp-11-9303-2011, 2011.

English, J. M., Toon, O. B., and Mills, M. J.: Microphysical simulations of large volcanic eruptions: Pinatubo and Toba, J. Geophys. Res., 118, 1880–1895, doi:10.1002/jgrd.50196, 2013.

Eyring, V., Lamarque, J.-F., Hess, P., Arfeuille, F., Bowman, K., Chipperfield, M. P., Duncan, B., Fiore, A., Gettelman, A., Giorgetta, M. A., Granier, C., Kinnison, M. H. D., Kunze, M., Langematz, U., Luo, B., Martin, R., Matthes, K., Newman, P. A., Peter, T., Robock, A., Ryerson, T., Saiz-Lopez, A., Salawitch, R., Schultz, M., Shepherd, T. G., Shindell, D., Staehelin, J., Tegtmeier, S., Thomason, L., Tilmes, S., Vernier, J.-P., Waugh, D. W., and Young, P. J.: Overview of IGAC/SPARC Chemistry-Climate Model Initiative (CCMI) Community Simulations in Support of Upcoming Ozone and Climate Assessments, in: SPARC Newsletter 40, p. 48–66, WMO/SPARC, Zürich, 2013.

Froyd, K. D., Murphy, D. M., Sanford, T. J., Thomson, D. S., Wilson, J. C., Pfister, L., and Lait, L.: Aerosol composition of the tropical upper troposphere, Atmos. Chem. Phys., 9, 4363–4385, doi:10.5194/acp-9-4363-2009, 2009.

Fueglistaler, S., Dessler, A. E., Dunkerton, T. J., Folkins, I., Fu, Q., and Mote, P. W.: Tropical tropopause layer., Rev. Geophys., 47, RG1004, doi:10.1029/2008RG000267, 2009.

Ghan, S. J. and Schwartz, S. E.: Aerosol properties and processes: A path from field and laboratory measurements to global climate models, Bull. Am. Meteor. Soc., 88(7), 1059–1083, doi:10.1175/BAMS-88-7-1059, 2007.

Gilman, D. L., Fuglister, F. J., and Mitchell Jr., J. M.: On the power spectrum of "red noise"., J. Atmos. Sci., 20, 182–184, 1963.

Giorgetta, M. A. and Bengtsson, L.: Potential role of the quasi–biennial oscillation in the stratosphere–troposphere exchange as found in water vapor in general circulation model experiments, J. Geophys. Res., 104, 6003–6019, 1999.

Giorgetta, M. A., Manzini, E., and Roeckner, E.: Forcing of the quasi–biennial oscillation from a broad spectrum of atmospheric waves, Geophys. Res. Lett., 29, 1245, doi:10.1029/2001GL014756, 2002.

Giorgetta, M. A., Manzini, E., Roeckner, E., Esch, M., and Bengtsson, L.: Climatology and forcing of the quasi–biennial oscillation in the MAECHAM5 model, J. Climate, 19, 3882–3901, 2006.

Grainger, R., Lambert, A., Rogers, C., Taylor, F., and Deshler, T.: Straospheric aerosol effective radius, surface area and volume estimated from infrared measurements, J. Geophys. Res., 100, 16 507 – 16 518, 1995.

Grant, W., Browell, E. V., Long, C. S., and Stowe, I. I.: Use of volcanic aerosols to study the tropical stratospheric reservoir, J. Geophys. Res., 101, 3973–3988, 1996.

Gray, L. J. and Chipperfield, M. P.: On the interannual variability of trace gases in the middle atmosphere, Geophys. Res. Lett., 17, 933–936, 1990.

Hamill, P., Toon, O. B., and Kiang, C. S.: Microphysical processes affecting stratospheric aerosol particles, J. Atmos. Sci., 34, 1104–1119, 1977.

Hamill, P., Jensen, E. J., Russel, P. B., and Bauman, J. J.: The life cycle of stratospheric aerosol particles, Bull. Am. Meteor. Soc., 78, 1395–1410, 1997.

Hasebe, F.: Quasi–biennial oscillations of ozone and diabatic circulation in the equatorial stratosphere, J. Atmos. Sci., 51, 729–745, 1994.

Hofmann, D., Barnes, J., O'Neill, M., Trudeau, M., and Neely, R.: Increase in background stratospheric aerosol observed with lidar at Mauna Loa Observatory and Boulder, Colorado., Geophys. Res. Lett., 36, L15 808, doi:10.1029/2009GL039008, 2009.

Hofmann, D. J.: Increase in the stratospheric background sulfuric acid aerosol mass in the past 10 years, Science, 248, 996–1000, 1990.

Holton, J. R., Haynes, P. H., McIntyre, M. E., Douglass, A. R., Rood, R. R., and Pfister, L.: Stratospheric–tropospheric exchange, Rev. Geophys., 33, 403–439, 1995.

Hommel, R.: Die Variabilität von stratosphärischem Hintergrund-Aerosol. Eine Untersuchung mit dem globalen sektionalen Aerosolmodell MAECHAM5-SAM2., Ph.D. thesis, Universität Hamburg, 2008.

Hommel, R., Timmreck, C., and Graf, H. F.: The global middle-atmosphere aerosol model MAECHAM5-SAM2: comparison with satellite and in-situ observations, Geoscientific Model Development, 4, 809–834, doi:10.5194/gmd-4-809-2011, 2011.

Höpfner, M., Glatthor, N., Grabowski, U., Kellmann, S., Kiefer, M., Linden, A., Orphal, J., Stiller, G., von Clarmann, T., Funke, B., and Boone, C. D.: Sulfur dioxide (SO_2) as observed by MIPAS/Envisat: temporal development and spatial distribution at 15–45 km altitude, Atmospheric Chemistry and Physics, 13, 10 405–10 423, doi:10.5194/acp-13-10405-2013, http://www.atmos-chem-phys.net/13/10405/2013/, 2013.

Horowitz, L. W., Walters, S., Mauzerall, D. L., Emmons, L. K., Rasch, P. J., Granier, C., Tie, X. X., Lamarque, J. F., Schultz, M. G., Orlando, G. S., and Brasseur, G. P.: A global simulation of tropospheric ozone and related tracers: Description and evaluation of MOZART, Version 2, J. Geophys. Res., 108, doi:10.1029/2002JD002853, 2003.

IPCC: Climate Change 2013: The Physical Science Basis. Contribution of Working Group I to the Fifth Assessment Report of the Intergovernmental Panel on Climate Change, Stocker, T.F. and D. Qin and G.-K. Plattner and M. Tignor and S.K. Allen and J. Boschung and A. Nauels and Y. Xia and V. Bex and P.M. Midgley (eds.), Cambridge University Press, Cambridge, United Kingdom and New York, NY, USA, 1535 pp., 2013.

Jacobson, M. Z.: Fundamentals of atmospheric modeling, Cambridge University Press, Cambridge, 2 edn., 68 pp., 2005.

Jöckel, P., Sander, R., Kerkweg, A., Tost, H., and Lelieveld, J.: Technical Note: The Modular Earth Submodel System (MESSy) - a new approach towards Earth System Modeling, Atmos. Chem. Phys., 5, 433–444, 2005.

Junge, C. E., Chagnon, C. W., and Manson, J. E.: Stratospheric aerosols, J. Meteorol., 18, 81–108, 1961.

Kasten, F.: Falling speed of aerosol particles., J. Appl. Meteorol., 7, 944–947, 1968.

Lin, S. J. and Rood, R. B.: Multidimensional flux form semi–Lagrangian transport, Mon. Wea. Rev., 124, 2046–2068, 1996.

Manzini, E., Giorgetta, M. A., Esch, M., Kornblueh, L., and Roeckner, E.: The influence of sea surface temperatures on the northern winter stratosphere: Ensemble simulations with the MAECHAM5 model, J. Climate, 19, 3863–3881, 2006.

Mills, M., Toon, O. B., and Solomon, S.: A 2D microphysical model of the polar stratospheric CN layer, Geophys. Res. Lett., 26, 1133 – 1136, 1999.

Mills, M., Toon, O., Vaida, V., Hintze, P., Kjaergaard, H., Schofield, D., and Robinson, T.: Photolysis of sulfuric acid vapor by visible light as a source of the polar stratospheric CN layer, J. Geophys. Res., 110, D08 201, doi:10.1029/2004JD005519, 2005.

Mote, P. W., Rosenlof, K. H., Mclntyre, M. E., Carr, E. S., Gille, J. C., Holton, J. R., Kinnersley, J. S., Pumphrey, H. C., Russell III, J. M., and Waters, J. W.: An atmospheric tape recorder: The imprint of tropical tropopause temperatures on stratospheric water vapor, J. Geophys. Res., 101, 3989–4006, 1996.

Murphy, D. M., Cziczo, D. J., Hudson, P. K., and Thomson, D. S.: Carbonaceous material in aerosol particles in the lower stratosphere and tropopause region, J. Geophys. Res., 112, D04 203, doi:10.1029/2006JD007297, 2007.

Naujokat, B.: An update of the observed quasi–biennial oscillation of the stratospheric winds over the tropics, J. Atmos. Sci., 43, 1873–1877, 1986.

Neely, R. R. I., English, J. M., Toon, O. B., Solomon, S., Mills, M., and Thayer, J. P.: Implications of extinction due to meteoritic smoke in the upper stratosphere, Geophys. Res. Lett., 38, L24 808, doi: 10.1029/2011GL049865, 2011.

Neely, R. R. I., Toon, O. B., Solomon, S., Vernier, J.-P., Alvarez, C., English, J. M., Rosenlof, K. H., Mills, M. J., Bardeen, C. G., Daniel, J. S., and Thayer, J. P.: Recent anthropogenic increases in SO2 from Asia have minimal impact on stratospheric aerosol, Geophys. Res. Lett., 40, 1–6, doi:10.1002/grl.50263, 2013.

Neu, J. L., Sparling, L. C., and Plumb, R. A.: Variability of the subtropical "edges" in the stratosphere, J. Geophys. Res., 108, 4482, doi:10.1029/2002JD002706, 2003.

Niemeier, U., Timmreck, C., Graf, H.-F., Kinne, S., Rast, S., and Self, S.: Initial fate of fine ash and sulfur from large volcanic eruptions, Atmospheric Chemistry and Physics, 9, 9043–9057, doi:10.5194/acp-9-9043-2009, 2009.

Pitari, G., Mancini, E., Rizi, V., and Shindell, D. T.: Impact of future climate and emission changes on stratospheric aerosols and ozone, J. Atmos. Sci., 59, 414–440, 2002.

Plumb, R. A. and Bell, R. C.: A model of quasibiennial oscillation on an equatorial beta–plane, Q. J. R. Meteorol. Soc., 108, 335–352, 1982.

Pruppacher, H. R. and Klett, J. D.: Micropysics of clouds and precipitation, D. Reidel, Dordrecht, 1979.

Rex, M., Timmreck, C., Kremser, S., Thomason, L., and Vernier, J.-P.: Stratospheric sulphur and its Role in Climate (SSiRC), in: SPARC Newsletter 39, p. 37, WMO/SPARC, Zürich, 2012.

Rinsland, C. P., Gunson, M. R., Ko, M. K. W., Weisenstein, D. W., Zander, R., Abrams, M. C., Goldman, A., Sze, N. D., and Yue, G. K.: H_2SO_4 photolysis: A source of sulfur dioxide in the upper stratosphere, Geophys. Res. Lett., 22, 1109–1112, 1995.

Roeckner, E., Baeuml, G., Bonaventura, L., Brokopf, R., Esch, M., Giorgetta, M., Hagemann, S., Kirchner, I., Kornblueh, L., Manzini, E., Rhodin, A., Schlese, U., Schulzweida, U., and Tompkins, A.: The atmospheric general circulation model ECHAM5 - Part I, Max Planck Institute for Meteorology, Hamburg, Germany, MPI Report No. 349, 2003.

Rosen, J. M.: The boiling point of stratospheric aerosols, J. Applied Meteor., 10, 1044–1045, 1971.

Sander, S., Friedl, R., Ravishankara, A., Golden, D., Kolb, C., Kurylo, M., Huie, R., Orkin, V., Molina, M., Moortgat, G., and Finlayson-Pitts, B.: Chemical Kinetics and Photochemical Data for Use in Atmospheric Studies, JPL Publication 06-2, Evaluation No 15, NASA Jet Propulsion Laboratory, California Institute of Technology, Pasadena, California, 2006.

Seinfeld, J. H. and Pandis, S. N.: Atmospheric chemistry and physics: From air pollution to climate change., 2nd ed., Wiley–Interscience, New York, 2006.

Seol, D.-I. and Yamazaki, K.: QBO and Pinatubo signals in the mass flux at 100 hPa and stratospheric circulation, Geophys. Res. Lett., 25, 1641–1644, 1998.

Society, R.: Geoengineering the climate. Science, governance and uncertainty., RS Policy Report 10/09, ISBN 978-0-85403-773-5, The Royal Society, London, 2009.

Solomon, S., Daniel, J. S., Neely, R. R., Vernier, J.-P., Dutton, E. G., and Thomason, L. W.: The Persistently Variable "Background" Stratospheric Aerosol Layer and Global Climate Change, Science, 333, 866–870, doi:10.1126/science.1206027, 2011.

SPARC/ASAP: WMO/SPARC Scientific Assessment of Stratospheric Aerosol Properties (ASAP), WCRP-124 WMO/TD- No. 1295, SPARC Report No. 4, edited by L. Thomason and Th. Peter, WMO, 2006.

Steele, H. M. and Hamill, P.: Effects of temperature and humidity on the growth and optical properties of sulfuric acid–water droplets in the stratosphere, J. Aerosol Sci., 12, 517–528, 1981.

Stier, P., Feichter, J., Kinne, S., Kloster, S., Vignati, E., Wilson, J., Ganzeveld, L., Tegen, I., Werner, M., Balkanski, Y., Schulz, M., Boucher, O., Minikin, A., and Petzold, A.: The aerosol–climate model ECHAM5–HAM, Atmos. Chem. Phys., 5, 1125–1156, 2005.

Thomason, L. W., Burton, S. P., Luo, B.-P., and Peter, T.: SAGE II measurements of stratospheric aerosol properties at non-volcanic levels, Atmos. Chem. Phys., 8, 983–995, 2008.

Timmreck, C.: Three–dimensional simulation of stratospheric background aerosol: First results of a multiannual general circulation model simulation, J. Geophys. Res., 106, 28 313–28 332, 2001.

Trepte, C. R. and Hitchman, M. H.: Tropical stratospheric circulation deduced from satellite aerosol data, Nature, 355, 626–628, 1992.

Turco, R. P., Hamill, P., Toon, O. B., Whitten, R. C., and Kiang, C. S.: A one–dimensional model describing aerosol formation and evolution in the stratosphere: I. physical processes and mathematical analogs, J. Atmos. Sci., 36, 699–717, 1979.

Vehkamäki, H., Kulmala, M., Napari, I., Lehtinen, K. E. J., Timmreck, C., Noppel, M., and Laaksonen, A.:

An improved parameterization for sulfuric acid water nucleation rates for tropospheric and stratospheric conditions, J. Geophys. Res., 107, 4622–4632, 2002.

Vernier, J.-P., Thomason, L. W., Pommereau, J.-P., Bourassa, A., Pelon, J., Garnier, A., Hauchecorne, A., Blanot, L., Trepte, C., Degenstein, D., and Vargas, F.: Major influence of tropical volcanic eruptions on the stratospheric aerosol layer during the last decade, Geophys. Res. Lett., 38, L12 807, doi: 10.1029/2011GL047563, 2011.

Vernier, J.-P., Thomason, L. W., Fairlie, T. D., Minnis, P., Palikonda, R., and Bedka, K. M.: Comment on "Large Volcanic Aerosol Load in the Stratosphere Linked to Asian Monsoon Transport", Science, 339, 647–d, 2013.

von Storch, H. and Zwiers, F. W.: Statistical analysis in climate research, Cambridge University Press, Cambridge, 1999.

Weisenstein, D. K., Yue, G. K., Ko, M. K. W., Sze, N.-D., Rodriguez, J. M., and Scott, C. J.: A two–dimensional model of sulfur species and aerosols, J. Geophys. Res., 102, 13 019–13 035, 1997.

Wurl, D., Grainger, R. G., McDonald, A. J., and Deshler, T.: Optimal estimation retrieval of aerosol microphysical properties from SAGE II satellite observations in the volcanically unperturbed lower stratosphere, Atmos. Chem. Phys., 10, 4295–4317, doi:10.5194/acp-10-4295-2010, 2010.

Yue, G., Poole, L., Wang, P.-H., and Chiou, E.: Stratospheric aerosol acidity, density, and refractive index deduced from SAGE II and NMC temperature data, J. Geophys. Res., 99, 3727–3738, 1994.

Appendix A

Table 1. Abbreviations.

ACE-FTS	Atmospheric Chemistry Experiment - Fourier Transform Spectrometer
AMIP2	Atmospheric Model Intercomparison Project
ASAP	Assessment of Stratospheric Aerosol Properties
ATMOS	Atmospheric Trace Molecule Spectroscopy
BDC	Brewer-Dobson Circulation
BHN	Binary Homogeneous Nucleation
CALIOP	Cloud-Aerosol Lidar with Orthogonal Polarisation
CCM	Chemistry Climate Model
CCMI	Chemistry-Climate Model Initiative
CCMVal	Chemistry-Climate Model Validation Activity
CTL	Control (experiment)
ECHAM	Acronym from ECMWF and Hamburg
ECMWF	European Centre for Medium Range Weather Forecasts
ERA	ECMWF Re-Analysis
ERBS	Earth Radiation Budget Satellite
HALOE	Halogen Occultation Experiment
ICAO	International Civil Aviation Organization
QBO	Quasi-Biennial Oscillation
MESSy	Modular Earth Submodel System
MIPAS	Michelson Interferometer for Passive Atmospheric Sounding
MOZART	Model for OZone And Related chemical Tracers
NASA	National Aeronautics and Space Administration
SAD	Surface Area Density
SAGE	Stratospheric Aerosol and Gas Experiment
SAM2	Stratospheric Aerosol Model version 2
SAO	Semi-Annual Oscillation
SMC	Secondary Meridional Circulation
SOLVE	SAGE III Ozone Loss and Validation Experiment
SPARC	Stratospheric Processes and their Role in Climate
TSR	Tropical Stratospheric Reservoir
TTL	Tropical Tropopause Layer
UT/LS	Upper troposphere and Lower Stratosphere
WMO	World Meteorological Organisation

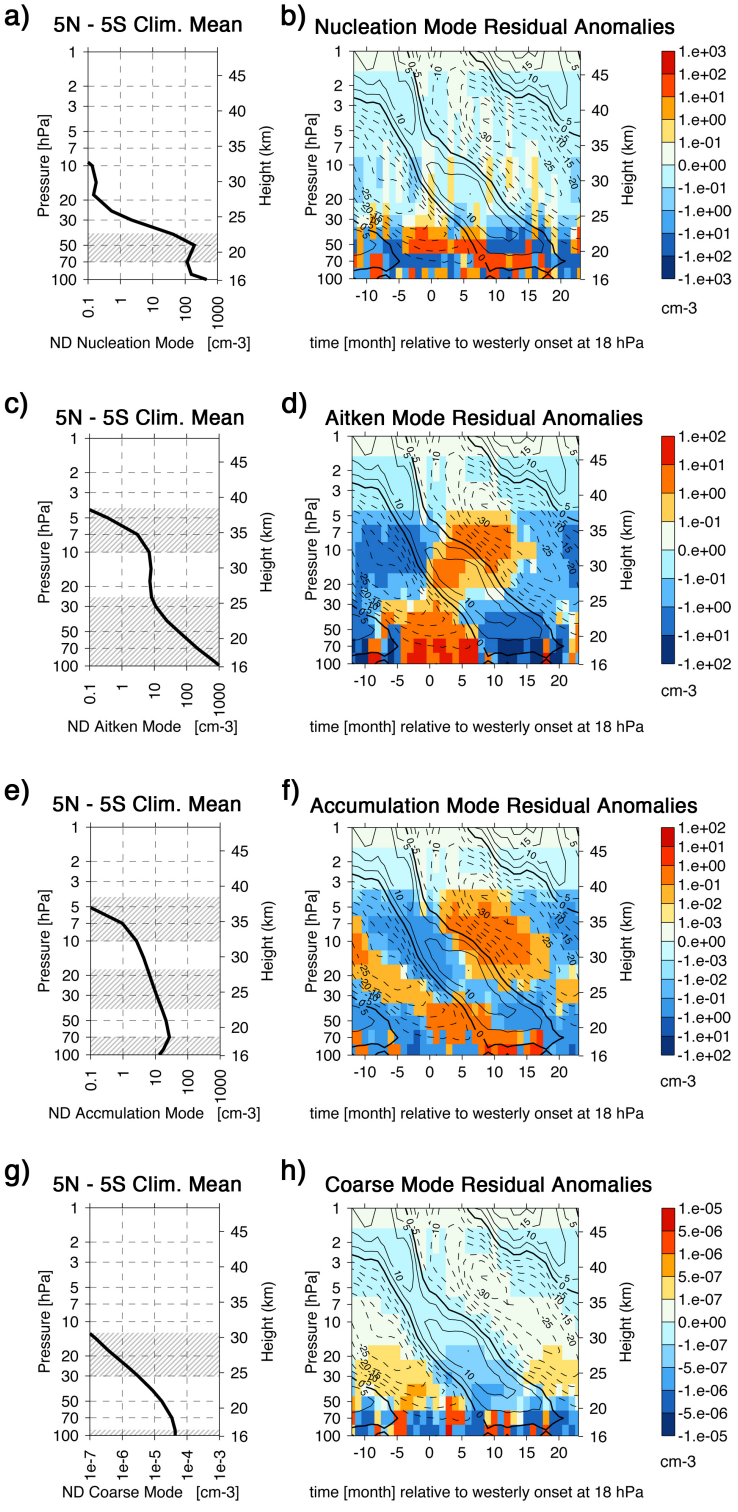

Fig. 10. As in Fig. 6, except for modelled number densities as integrals over specified modes: (a) and (b) nucleation mode ($R < 0.005\,\mu\text{m}$), (c) and (d) Aitken mode ($0.005\,\mu\text{m} \leq R < 0.05\,\mu\text{m}$), (e) and (f) accumulation mode ($0.05\,\mu\text{m} \leq R < 0.5\,\mu\text{m}$), and (g) and (h) coarse mode ($R \geq 0.5\,\mu\text{m}$).

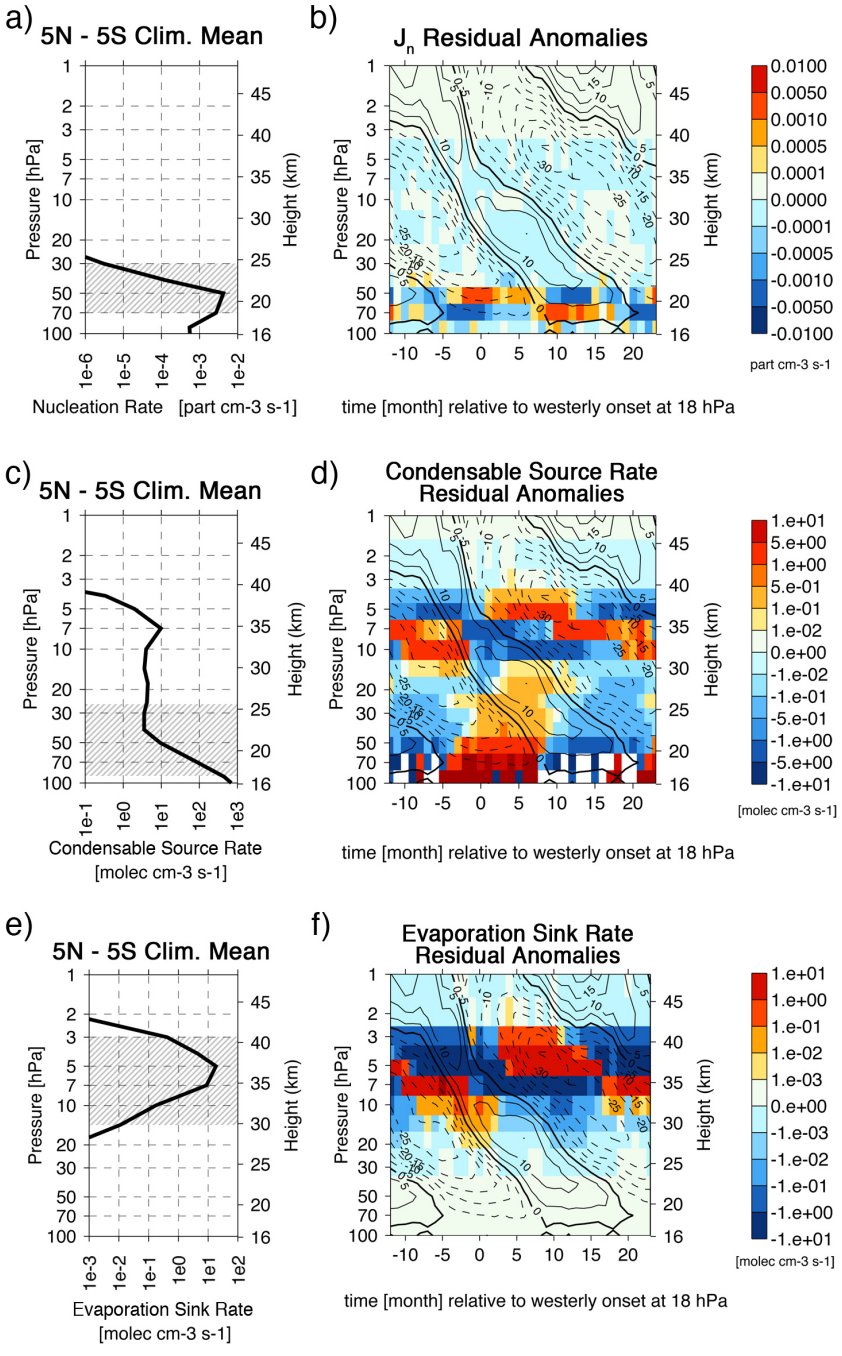

Fig. 11. As in Fig. 6, except for modelled microphysical processes. The upper panel shows the binary homogeneous nucleation rate ($\mathrm{cm^{-3}\,s^{-1}}$) as parametrised by Vehkamäki et al. (2002)~~, the middle panel the time-averaged vapour concentration () that condenses onto aerosols. The bottom panel shows the time-averaged vapour concentration () that evaporats from aerosols~~. **The middle panel shows the time-averaged condensable source rate of $\mathbf{H_2SO_4}$ vapour ($\mathbf{cm^{-3}\,s^{-1}}$) and the bottom panel the respective counterpart, the time-averaged evaporation sink rate of $\mathbf{H_2SO_4}$ molecules ($\mathbf{cm^{-3}\,s^{-1}}$).**

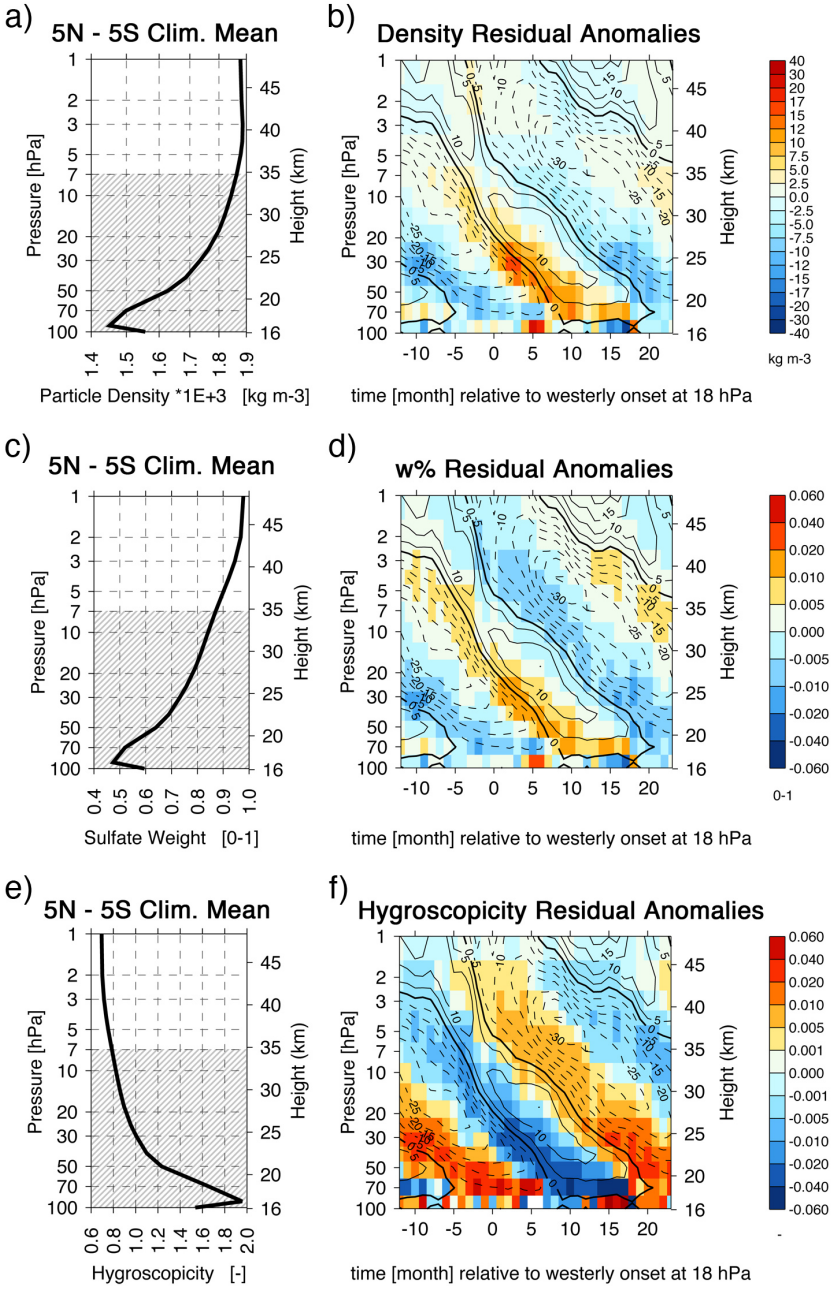

Fig. 12. As in Fig. 6, except for modelled sulphate aerosol properties. The upper panel shows the density of the binary $H_2SO_4-H_2O$ solution, the middle panel the H_2SO_4 weight percentage, and the bottom panel the aerosol water content relative to a representative Junge layer aerosol composition (e.g. Rosen, 1971).

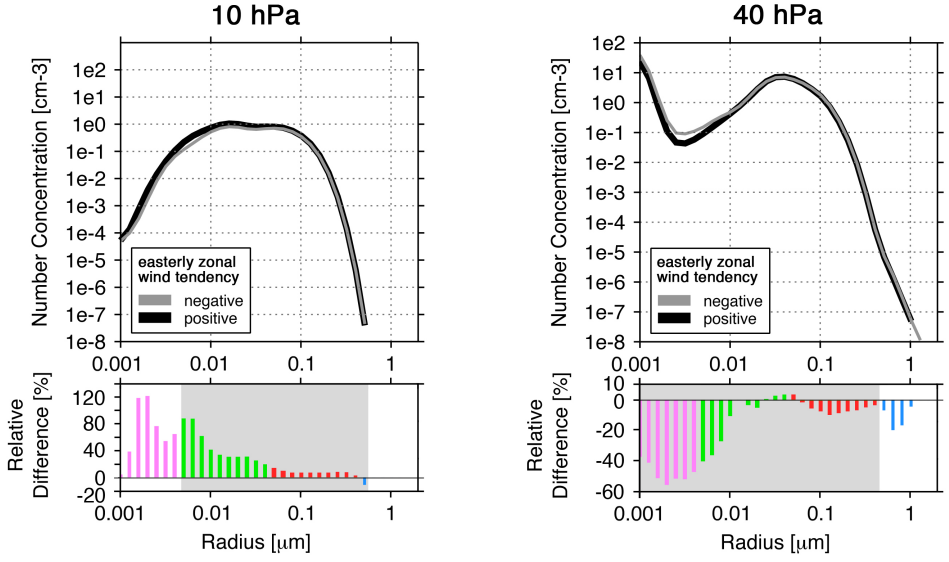

Fig. 13. Comparison of modelled aerosol size distributions and associated QBO modulations, exemplarily at the 10 and 40 hPa pressure

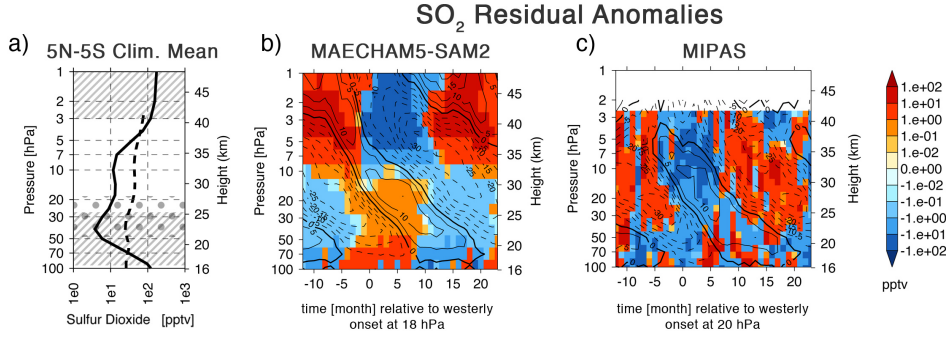

Fig. 14. ~~As in Fig. 6, except for prognostic sulphate aerosol precursor gases. The upper panel shows the mass mixing ratio, the middle panel the mass mixing ratio, and the bottom panel the mass mixing ratio.~~ Comparison between the modelled SO_2 mass mixing ratio and Envisat/MIPAS observations from Höpfner et al. (2013) . (a) climatologic

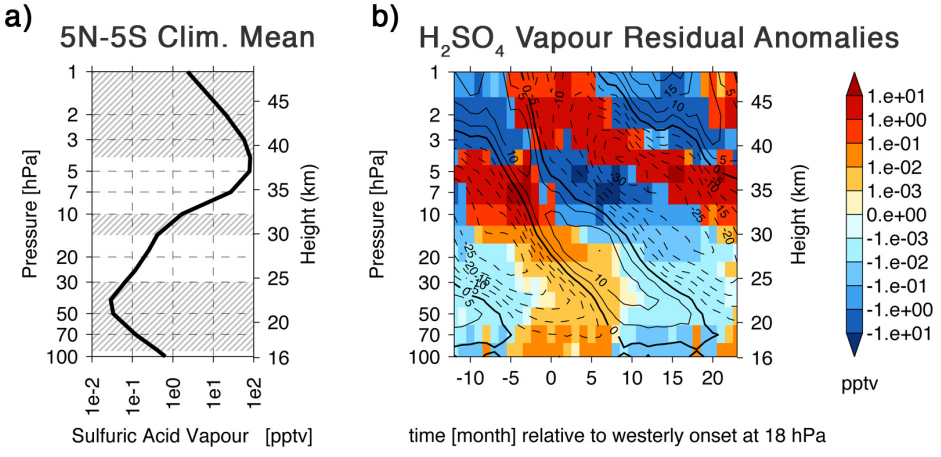

Fig. 15. As in Fig. 6, except for the modelled H_2SO_4 vapour mass mixing ratio.